Chapter

Physical Volcanology and Facies Analysis of Silicic Lavas: Monte Amiata Volcano (Italy)

Luigina Vezzoli, Claudia Principe, Daniele Giordano, Sonia La Felice and Patrizia Landi

Abstract

Monte Amiata (Italy) is a middle Pleistocene silicic volcano characterized by the extrusion of extensive (5–8 km long and 60 m thick on average) sheet-like lava flows (SLLFs). It is one of the prime volcanoes that have been involved in the volcanological debate on the genetic interpretation of large silicic flows. We performed integrated stratigraphic, volcanological, and structural field survey and petrochemical study of Monte Amiata SLLFs to describe their volcanic facies characteristics and to elucidate their eruptive and emplacement processes. Individual flow units exhibit basal autoclastic breccia beds or shear zones, frontal ramp structures, massive cores with subvertical cooling columnar jointing, coherent non-vesicular upper parts, and plain surfaces with pressure ridges. Internal shear-bedding and crystals and vesicles lineations define planar to twisted and straightened outflow layering. The absence of fragmental textures, both at micro- and macro-scale, supports the effusive nature for the SLLFs. The most common lithology is a vitrophyric trachydacite of whitish to light-gray color, showing a homogeneous porphyritic texture of K-feldspar, plagioclase, pyroxene, and biotite, in a glassy perlitic or microcrystalline poorly vesicular groundmass. Morphological features, facies characteristics, internal structure, and petrographic textures of these silicic sheet-like and long-lasting flows suggest that their effusive emplacement was governed by peculiar physicochemical and structural conditions.

Keywords: sheet-like silicic lava flow, volcanic facies, emplacement dynamics, volcano-tectonics, perlite, Monte Amiata

1. Introduction

Due to their relatively high viscosity and volatile content, silicic (SiO_2 > 63 wt%) magmas are mainly erupted explosively producing voluminous fallout and ignimbrite deposits, which can reach areal extension of thousands of square kilometers and thickness of hundreds of meters (e.g., [1]). In contrast, silicic effusive eruptions are correlated with domes and short and thick flows. The emplacement of silicic lavas is commonly governed by physical variables such as the high viscosity, low temperature

and volatile content, and low eruption rates. Moreover, silicic lava effusions are poorly constrained because of a paucity of direct observations on historical eruptions (i.e., Colima, Mexico, 1998–1999, [2]; Santiaguito, Guatemala, 1922 to present, [3]; Chaitén, Chile, 2008–2009, [4]; Cordón Caulle, Chile, 2011–2012, [5–7]). Overall, the best known and described silicic effusive products are rhyolite lava domes [8] and stubby obsidian flows restricted to the near-vent areas [9, 10]. Since the 1960s, more extensive silicic volcanic units have been the object of controversy over their origin because of volcanological characteristics typical of either lava flows and welded or rheomorphic pyroclastic rocks (ignimbrite). In more recent times, several of these extensive sheet-like silicic volcanic units were interpreted as lava flows and distinguished from rheomorphic ignimbrites in well-documented geological records worldwide [11–21]. However, some key questions regarding the eruption and emplacement mechanisms of large volume silicic lavas remain still open [22–25].

Monte Amiata is a silicic (mainly trachydacite) middle Pleistocene volcano (**Figure 1**) of the Tuscan Magmatic Province (Italy; [26]) that focused on the interest of volcanologists and petrologists for about 300 years since the eighteenth century [27] and was one of the prime volcanoes that have been involved in the volcanological debate on the genetic interpretation of the enigmatic sheet-like silicic volcanic rocks [28–33].

Monte Amiata is that volcano for which the word "rheoignimbrite" was first coined by Alfred Rittmann [30] to indicate a volcanological process explaining the concomitant lava- and pyroclastic-like textural and geological characteristics found in some silicic volcanic rocks [33]. The pristine interpretation of Monte Amiata ignimbrites and rheoignimbrites by Rittmann was not universally accepted (e.g., [34]; G.P. L. Walker in [32]). However, the concept of rheomorphism, considered such as a post-depositional gravitational flow and deformation process, has been subsequently recognized and applied in volcanology to ignimbrites (e.g., rheomorphic ignimbrites; [35, 36]), pyroclastic fall deposits [32], and lavas. After the Rittmann assumption, the various studies present in the literature [37–44] have in fact suggested not conclusive data and interpretations about the eruption processes of Monte Amiata silicic rocks, mainly because of the lack of exhaustive physical volcanological observations and their interpretations in a modern volcanological framework.

Nowadays, we accept that Monte Amiata is a completely effusive silicic volcano whose activity was dominated by the emplacement of silicic lava flows, exogenous lava domes, and coulées [45]. To support our interpretation, we have performed

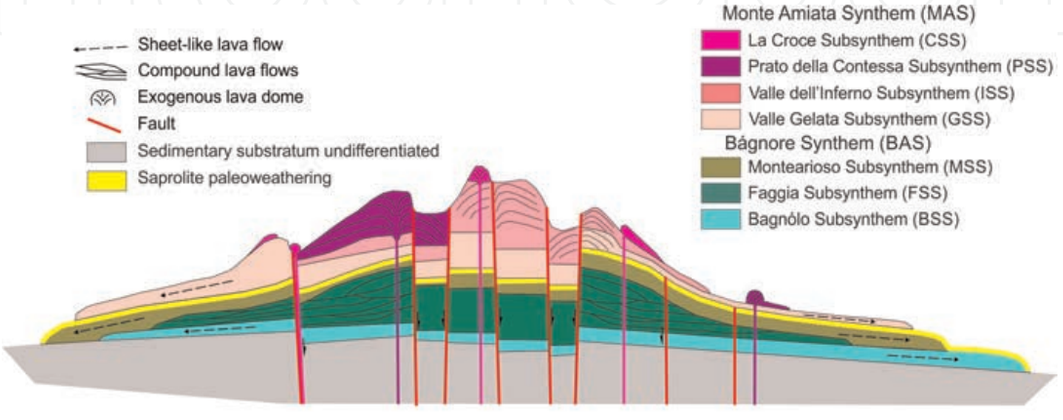

Figure 1.
Idealized cross section showing the stratigraphic relationships and the internal architecture of the completely effusive silicic Monte Amiata composite volcano. Not in scale.

detailed and systematic field-based investigations on the stratigraphy, structure, physical features, volcanic facies, and macroscopic and microscopic structures and textures of Monte Amiata deposits.

Specifically, this chapter focuses on several sheet-like lava flows (SLLFs) that constitute the main part of the Monte Amiata volcanic edifice and offer an excellent opportunity to learn more about extensive and voluminous silicic lavas. The goals of our study are (1) to discuss some criteria to distinguish silicic lava flows from welded tuffs and rheoignimbrites, (2) to interpret ascent, eruption, and emplacement mechanisms for Monte Amiata trachydacite through physical and observational data, (3) to produce a model of emplacement for the SLLFs, and (4) to suggest reading keys for the interpretation of the eruptive activity, which originates for such kind of magmatic, structural, and volcano-tectonic environments. We are convinced that the conclusions obtained for Monte Amiata can be applied to improve the general understanding of the volcanic processes at the origin of the emplacement of large silicic effusive bodies and to enhance the assessment of their associated volcanic hazard.

2. Geological setting

2.1 Overview of Monte Amiata volcano

Monte Amiata (42°53′15″N, 11°37′24″E) is a middle Pleistocene polygenetic volcano culminating at 1738 m above sea level (a.s.l.) and located in southern Tuscany (Italy) within the Tuscan Magmatic Province [26]. The province formed in the inner sector of the Late Cretaceous–Early Miocene Northern Apennine thrust-and-fold belt [46, 47] and appears related to crustal thinning and asthenosphere upwelling [48, 49] associated with a Miocene-Pleistocene extensional tectonic regime [50, 51] that favored the partial melting in lower crust and mantle [26]. Magmatism in the province extended from 8 Ma to 0.2 Ma and includes plutonic and volcanic rocks. Monte Amiata is the youngest volcanic activity of the province. Its volcanic products overlay a sedimentary substratum represented by marly limestones and calcareous sandstones of Mesozoic-Cenozoic age [52].

Monte Amiata was active in a short interval of time (305–231 ka, [53, 54]). The source vents are eruptive fissures forming a 7 km-long, NE-SW-trending volcanic rift zone (**Figures 1** and **2**; [45]) related to a regional transtensional fault system (Bágnore—Bagni S. Filippo Shear Zone; [55]). Times and modes of the volcanic activity and evolution, such as the volcano-tectonic deformations of the edifice and the periodic refilling of the shallow silicic reservoir with new basaltic magmas ([56], and references therein), were probably controlled by the tectonic deformations along this shear zone [45].

The main composition of Monte Amiata lavas is trachydacite, with subordinate latite [40, 42, 44, 57]. Mafic magmatic enclaves (ME) are present within the silicic lava flows [58] and reflect the indirect mantle input to the volcanic activity and geological evolution [44, 45].

Based on a new accurate stratigraphic and structural geological survey [45, 59–62], we have innovatively proposed that the Monte Amiata geological evolution consists of two main periods of activity corresponding to two Unconformity Bounded Stratigraphic Units (UBSUs; [63]): the older Bágnore Synthem (BAS) and the younger Monte Amiata Synthem (MAS) (**Figure 1**). They are separated by a period of volcanic quiescence represented by a major geological unconformity during which a surface of intravolcanic saprolite paleo-weathering and associated tectonic deformations

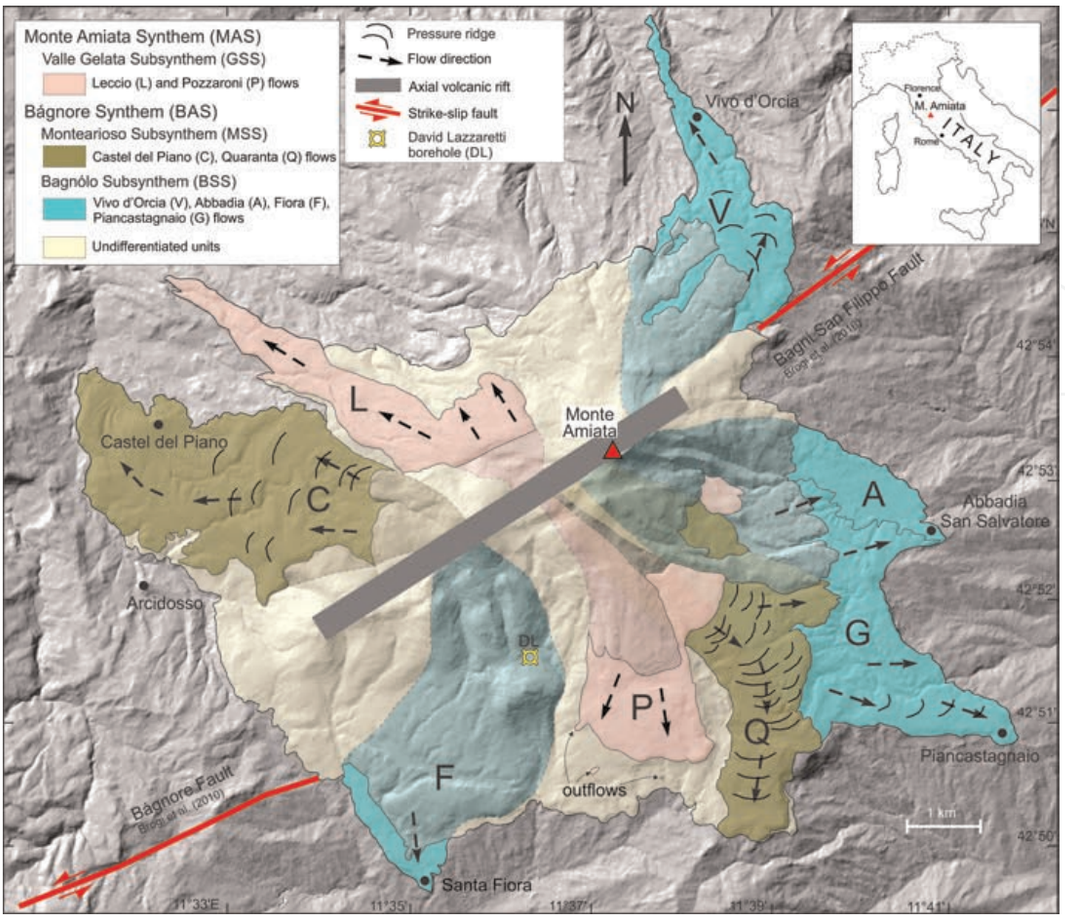

Figure 2.
*Geologic sketch map of Monte Amiata showing the sheet-like lava flows (SLLFs) object of the study. The last phases of activity (Valle dell'Inferno, Piano della Contessa, and La Croce Subsynthems; see **Figure 1**), which not include SLLFs, are omitted. Colors of stratigraphic units are as in **Figure 1**. The more intense color tone indicates exposed SLLFs, and the lighter one indicates the inferred portions covered by younger units. Letters for name of SLLFs: A—Abbadia San Salvatore, C—Castel del Piano, F—Sorgente del Fiora, G—Piancastagnaio, P—Pozzaroni, Q—Quaranta, V—Vivo d'Orcia. The presence of ogive structure on some flow surface is depicted. Front and margins of the Pozzaroni lava flow show outflow lobes. Geologic mapping from your original field survey. Digital terrain model (DEM) basis from the technical map of the Tuscany Region at the 1: 10,000 scale.*

developed at expense of the BAS rocks [62]. Then, the recognition of other surfaces of discontinuity of lower rank has made it possible to divide these two synthems into seven subsynthems (**Figure 1**). Monte Amiata succession does not record pyroclastic deposits, on the contrary to common composite silicic volcanoes that show packages of intercalated tuffs and lava flows.

From its earliest stages, BAS volcanic activity is characterized by the emplacement of several extensive, individual SLLFs (Bagnólo Subsynthem-BSS; **Figure 1**) that flowed N, SE, and S for very long distances (up to 8 km) and crop out in the distal portion of the volcanic edifice (**Figure 2**; [45]). After the construction of an effusive cone formed by the successive emplacement and overlap of channelized compound lava flows (Faggia Subsynthem-FSS; **Figure 1**), more localized individual SLLFs are once again extruded (Montearioso Subsynthem-MSS; **Figures 1** and **2**; [45]). Younger units, composing MAS, comprise long individual SLLFs that reach 5–6 km in length (**Figure 2**) associated with extrusive lava domes and coulées (Valle Gelata Subsynthem-GSS; **Figure 1**), followed by numerous exogenous lava domes with associated coulées (Valle dell'-Inferno-ISS and Prato della Contessa-PSS Subsynthems) and, finally, by some smaller channelized lava flows (La Croce Subsynthem-CSS; **Figure 1**; [45]).

2.2 Previous studies and open questions

Two fundamental geological problems on Monte Amiata volcano emerged from previous studies carried out during the last 60 years including the issues associated with the correct definition of the stratigraphic units and, consequently, of the interpretation of the geological evolution in light of the revised volcanological interpretation of the eruption dynamics and the emplacement processes.

In all previous studies, the reconstruction of the stratigraphic framework was founded mainly on lithological and petrographic characteristics rather than on objective geological criteria applying the principal approach of volcano geology. Consequently, based on supposedly homogeneous and indistinguishable textures, geochemical composition, and mineral paragenesis of rocks, the resulting volcanic history was represented by only three units [39, 40, 43]. This tri-fold division of the volcanic activity of Monte Amiata includes (1) an initial and single extended sheet of vitrophyric flows (Basal Complex Auctorum), (2) a cluster of lava domes and coulées extruded from the axial summit crest of the volcano, and (3) two final trachyandesite (olivine-phyric latite) small lava flows.

In fact, in all previous studies on Monte Amiata, the SLLFs of the lower portion of the stratigraphic succession (Basal Complex Auctorum) were all assigned to a single eruptive event (in turn explosive, effusive, or mixed), which would have marked the beginning of the activity of the volcano. Differently, the stratigraphic reconstruction presented in our works ([45, 59–62], this paper) demonstrates that the SLLFs are not a large indistinct unit produced by a single eruptive event, but that they consist of numerous eruptive units that are distinct in the source area, areal distribution, and volcanological and petrographic features. Moreover, these single eruptive units until now included in the former Basal Complex Auctorum are actually individual lithostratigraphic units found at different levels of the stratigraphic succession (**Figures 1** and **2**).

After the initial definition as ignimbrites and rheoignimbrites [30, 37–39], the genetic interpretation of the extensive sheet-like trachydacite flows of Monte Amiata has been the subject of various conjectures, which, however, was not supported by stratigraphic and structural field data and by an accurate volcanological definition of the depositional facies. Ref. [40] proposed a mixed complex eruption, with an initial explosive phase followed by an effusive phase. The effusive nature of these flows has been generically supposed by various authors [41, 42], albeit in contexts focused on other topics and without any objective observation. Refs. [43, 44] proposed a highly speculative mechanism of the collapse of an endogenous summit mega-dome generating a single predominantly gravitational flow of fragmented and still hot material that was distributed all around the volcano and evolved in a rheomorphic sheet, which flowed like lava after emplacement.

On the basis of the various physical and compositional indicators, stratigraphic relations, and our geologic mapping, we do not agree with these previous interpretations for any of the Monte Amiata sheet-like trachydacite flows.

3. Materials and methods

This chapter focuses on the volcanological and stratigraphic characterization and interpretation of the SLLFs of Monte Amiata volcano. The stratigraphic identification and cartography of the geological units studied are based on the stratigraphic criteria of the Unconformity Bounded Stratigraphic Units (UBSUs; [63]), following the

suggestions of the International Stratigraphic Guide (that can be accessed online http://www.stratigraphy.org). This type of stratigraphic unit is defined as a rocky body bounded to the top and bottom by specific, significant, and demonstrable surfaces of geologic discontinuity. The basic synthem unit can be divided into two or more subsynthems. Names of units adopted in this work have been introduced and described in previously published papers [45, 62].

The description of lava flows studied is based on the analysis of volcanic facies [64, 65]. For depositional facies, we mean the set of lithological characters of a rock, which allows its distinction according to some combination of physical features and composition, without nor genetic neither stratigraphic significance. Different facies record variations in conditions and processes of formation and deposition; consequently, they can lead to the interpretation of volcanological genetic processes and emplacement mechanisms. For each of the identified volcanic facies, we describe physical and morpho-structural features, internal and surface structures, and macroscopic and microscopic textures, and we propose their genetic interpretation. The internal arrangement of facies in terms of vertical and horizontal sequence and association contributes to recognize the architecture of the effusive volcano. We refer to a flow unit as the deposit of a discrete flow within an eruption event, whereas to an eruptive unit as all the products effused during a time- and space-distinct eruption event which can also be composed of several successive flow units. Individual eruptive unit outlines have been delineated and mapped from field evidence, and patterns and textural differences.

The petrographic observation of the Monte Amiata rock samples allowed to recognize several different exposed lithotypes [57] on the basis of different paragenesis, groundmass textures, and content in mafic magmatic enclaves and meta-sedimentary xenoliths. About 30 rock samples belonging to the SLLFs discussed in this work were analyzed under a polarizing microscope at Institute of Geosciences and Earth Resources (National Research Council of Italy), Pisa (Italy), in order to carry out a textural, petrographic, and mineralogical characterization. In addition, further textural investigations were performed at the National Institute of Geophysics and Volcanology (INGV), Pisa (Italy), using a Zeiss EVO MA 10 Scanning Electron Microscope (SEM), capturing selected back-scattered electron (BSE) images.

The morphometric parameters of Monte Amiata lava flows were determined in the field and with reference to the geologic map (**Figure 2**; see also [45]). The area, minimum length, and slope of each flow were calculated by means of the ruler tool of Google Earth on the basis of the performed geological mapping. The average thickness of each eruptive unit was estimated from outcrop relief scaled from the topographic base maps. Most calculated volumes are less than real volumes because a great part of the SLLFs are covered by the overlying volcanic units, and their extent to the source zone is actually unknown. Anyway, the calculated volume is essentially a dense-rock equivalent, since porosity in these lavas is generally very low to absent.

4. Results on Monte Amiata trachydacite SLLFs

4.1 Stratigraphic relationships and physical features

The long, trachydacite SLLFs span over the stratigraphic succession of the volcano and are not restricted to a particular stratigraphic level (**Figure 1**). They are more abundant but not exclusive in Bágnore Synthem (BAS), as they are found also in Monte Amiata Synthem (MAS).

Among the BAS trachydacite, we have identified two stratigraphically distinct groups of SLLFs. The oldest SLLFs group crops out at the base of the volcanic stratigraphic sequence (BSS; **Figure 1**) and comprises the Sorgente del Fiora, Piancastagnaio, Abbadia San Salvatore, and Vivo d'Orcia lithostratigraphic and eruptive units (**Figure 2**). They spread NW and SE over a wide area unconformably overlying the pre-volcanic sedimentary substratum and are extensively exposed along the external perimeter of the volcano. They reach distances up to 5–8 km from the probable vent area, with widths up to 1.5–2 km and thickness of 30–90 m (**Table 1**). A second BAS series of SLLFs (MSS; **Figure 1**) is in the NW and S sides of the edifice and comprises the Castel del Piano and Quaranta lithostratigraphic and eruptive units (**Figure 2**). They reached a distance of about 7 km from the probable emission centers, with thicknesses of 50–80 m (**Table 1**). After an interval of weathering (saprolite) and faulting, the resumed MAS volcanic activity (GSS; **Figure 1**) produced extensive SLLFs along the N and S slopes forming Leccio and Pozzaroni lithostratigraphic and eruptive units (**Figure 2**) with length of 5–6 km and thickness ranging 50–70 m (**Table 1**).

The two younger SLLFs (GSS; Leccio and Pozzaroni) show about the same area (5–6 km^2) that is the smallest of the Monte Amiata SLLFs. The greatest extent (10–11 km^2) is reached by the SLLFs of MSS (Quaranta and Castel del Piano). Intermediate areas (7–9 km^2) are typical of SLLFs effused during BSS, considering in this case the incertitude in vent positioning and the related error in the area calculations (**Table 1**).

The calculated average volume of the SLLFs spans between 0.30 and 0.72 km^3. To be considered that the error associated with these volumes is quite high, with the exception of Pozzaroni and Leccio SLLFs (**Figure 3a**), due to the incertitude on the thickness distribution along the lava flow's path. There is a faint linear correlation between the calculated volumes and the flows lengths (R: 0.423) (**Table 1** and **Figure 3a**). Moreover, two different alignments are recognizable in both area/length and volume/length graphs (**Figure 3a** and **b**). In particular, (i) there is a very good linear correlation (R: 0.994) between both volume and area and the length of the three

SLLF	Label	S/SS	Area (km^2)	Length (km)	Slope (%)	Thickness range (m)	Average thickness (m)	Volume (km^3)	Average volume (km^3)
Pozzaroni	P	MAS/GSS	5.83	4.75	9.7	70–50	60	0.41–0.29	0.35
Leccio	L	MAS/GSS	5.00	6.33	18.6	70–50	60	0.35–0.25	0.30
Quaranta	Q	BAS/MSS	9.98	6.94	13.0	80–50	65	0.80–0.50	0.65
Castel del Piano	C	BAS/MSS	11.23	7.00	5.3	80–50	65	0.90–0.56	0.73
Piancastagnaio	G	BAS/BSS	8.66	7.72	13.2	90–30	60	0.78–0.26	0.52
Fiora	F	BAS/BSS	9.76	5.57	11.2	90–30	60	0.88–0.29	0.59
Abbadia	A	BAS/BSS	7.36	5.07	8.0	90–30	60	0.66–0.22	0.44
Vivo d'Orcia	V	BAS/BSS	6.50	6.76	9.2	90–30	60	0.59–0.20	0.39

*Slope is average from the inferred vent to the terminus of the flow. S: synthem, SS: subsynthem, and labels of eruptive units as in **Figure 2**.*

Table 1.
Morphometric parameters for the sheet-like lava flow (SLLF) of Monte Amiata.

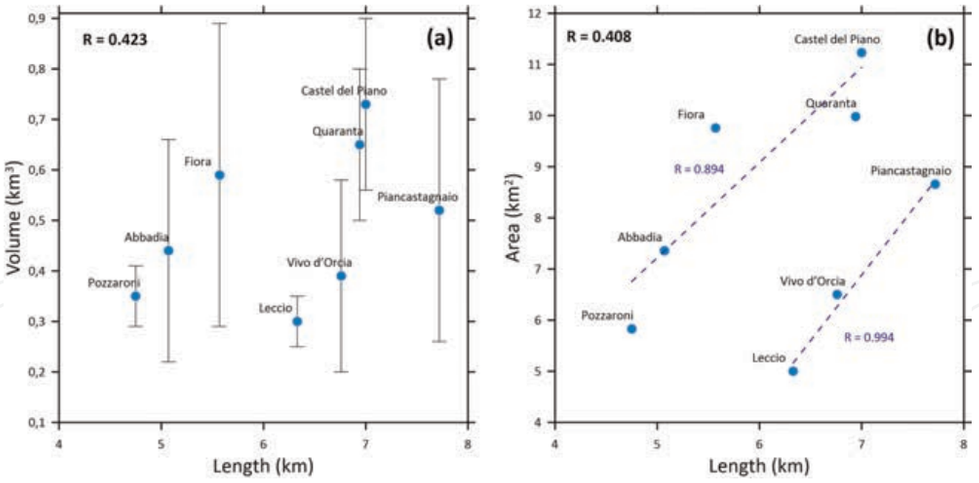

Figure 3.
Plots (a) length vs. volume and (b) length vs. area for the Monte Amiata SLLFs. R is the linear correlation coefficient. See text for explanation.

valley-controlled lava flows of Leccio, Vivo d'Orcia, and Piancastagnaio (in its terminal portion), and (ii) a quite good linear correlation (R: 0.894) for the other five lava flows that distributed in larger lava bodies. In this last case, the poor correlation can be attributed to the exposure condition of the lava flows that influence the accuracy of the area calculation. No correlation is observed between area and slope values, suggesting that the different areal distribution of SLLFs can be independent of the underlying morphology [66], but depending probably on the physicochemical properties of the erupted magma (see discussion in Section 5.2).

The present topographic surface of Monte Amiata volcano represents the primary volcanic surface of the subsequent constructional bodies that concurred to build the volcanic edifice, with the little effects of exogenous erosion and tectonic deformation. All SLLFs are characterized by low- or moderate-relief surfaces forming large tabular areas on the slopes of Monte Amiata. Different lava plateaus developed at different altitudes and formed a stepped relief consisting of overlapping plains separated by breaks of slope [45, 62]. This morphology suggests that flows were not confined by channels and spread along the low-relief sides of the volcano. In the case of Vivo d'Orcia (BAS) and Leccio (MAS) eruptive units (**Figure 2**), lavas moved down the outer flank of the volcano following tectonically controlled preexisting drainage, entering and filling river furrows where they stopped.

The source areas of SLLFs are mainly buried by younger volcanic units and probably correspond to the present elongated summit crest of the volcano (**Figure 2**). Exposures of the flows are largely their surficial part; abrupt but irregular scarps identify the flow fronts and margins. Due to the relatively old age of the volcano, the outcrops are subject to possible surface erosion and front collapses (for this reason, the measured lava length and area have to be considered as minimum values) and the exposed logs are often discontinuous.

The opportunity to access to the complete succession of a SLLF was a continuously cored deep borehole (David Lazzaretti borehole; [67–69]) that intersected top-to-bottom the Sorgente del Fiora eruptive unit. This drilling is located on the southern slope of the volcano about 2 km NNE of the lava flow front (DL in **Figure 2**) and displays well-preserved lithofacies and internal textures. The Sorgente del Fiora lava was recovered between 147 m and 265 m of depth from the ground level (i.e., between 939 and 821 m a.s.l.) and shows a thickness of 118 m (**Figure 4a**). It overlies a lower

volcanic sequence of trachydacite predating the exposed units and is overlain by trachydacite belonging to FSS.

4.2 Lithofacies, structures, and textures

4.2.1 Macroscopic lithofacies and facies association

Based on observations of outcrops, hand specimens, and drill cores in the Monte Amiata SLLFs trachydacite (**Figure 4**), we have identified four main coherent lithofacies based on variations in groundmass texture, color, and vesicularity. In addition, three fragmental lithofacies have also been recognized based on differences in texture and composition of clasts and matrix. In all these lithofacies, trachydacite is characterized by nearly identical mineral paragenesis (K-feldspar, plagioclase, biotite, and subordinate pyroxene) and phenocrysts size. The characteristics of these lithofacies and their facies association are well exemplified by the lithostratigraphic log of the Sorgente del Fiora eruptive unit in the David Lazzaretti borehole compared with the correlate outcropping sequence (**Figure 4**).

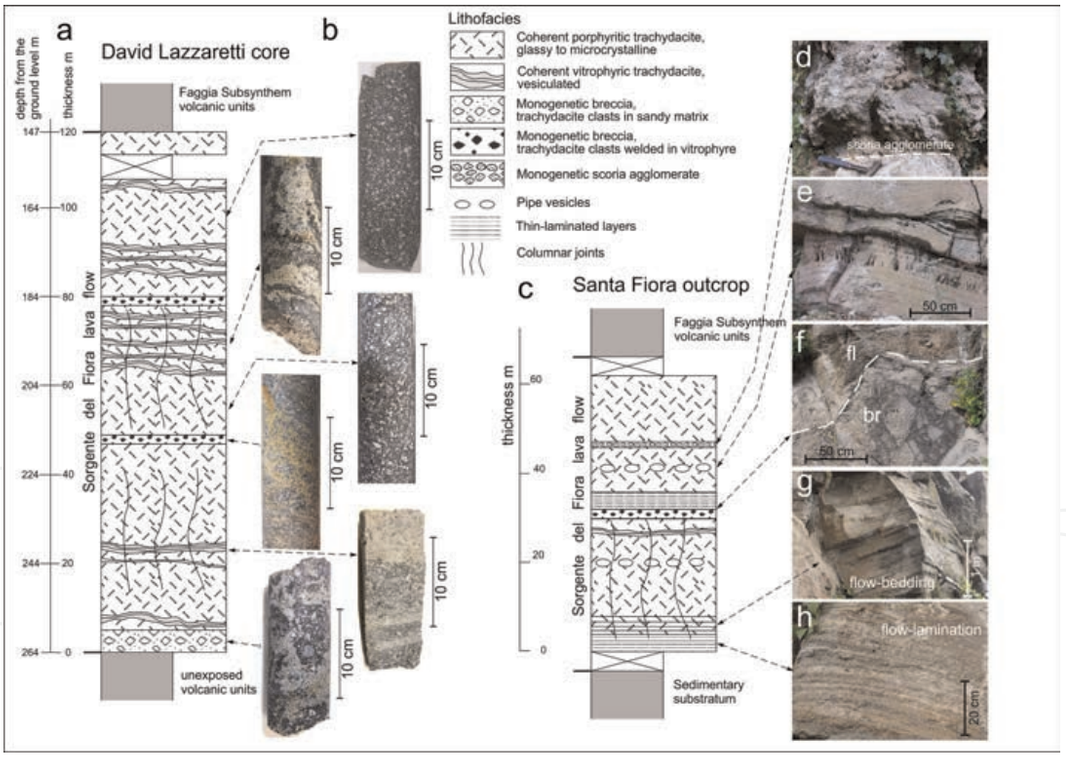

Figure 4.
The Sorgente del Fiora eruptive unit is representative of the trachydacite SLLFs of Monte Amiata, showing the vertical distribution and association of the coherent and fragmental lithofacies identified. (a) Lithostratigraphy of the drill core David Lazzaretti (DL in ***Figure 2****) that intersected top-to-bottom the Sorgente del Fiora unit. (b) Examples of the main lithofacies identified and described in the DL core. (c) Generalized lithostratigraphic log through the Sorgente del Fiora unit from outcrops along flow margins and front. (d) Interflow scoria agglomerate (lithofacies g). Hammer for scale. (e) Vesicle layering. Some beds show tubular vesicles a few cm high. In the upper right part of the image, flow bands have been deflected around a lens of coarse vesiculation, implying that the vesicles formed while the lava was still ductile, probably during flowage. (f) Interflow monogenetic breccia with welded vitrophyric matrix (br; lithofacies f) overlain by thin-laminated lava beds (fl). (g) Flow bedding composed of massive porphyritic lava beds separated by sheet joints. (h) Thin flow lamination alternating massive porphyritic, vesicular, and glassy lava layers at mm to cm scale.*

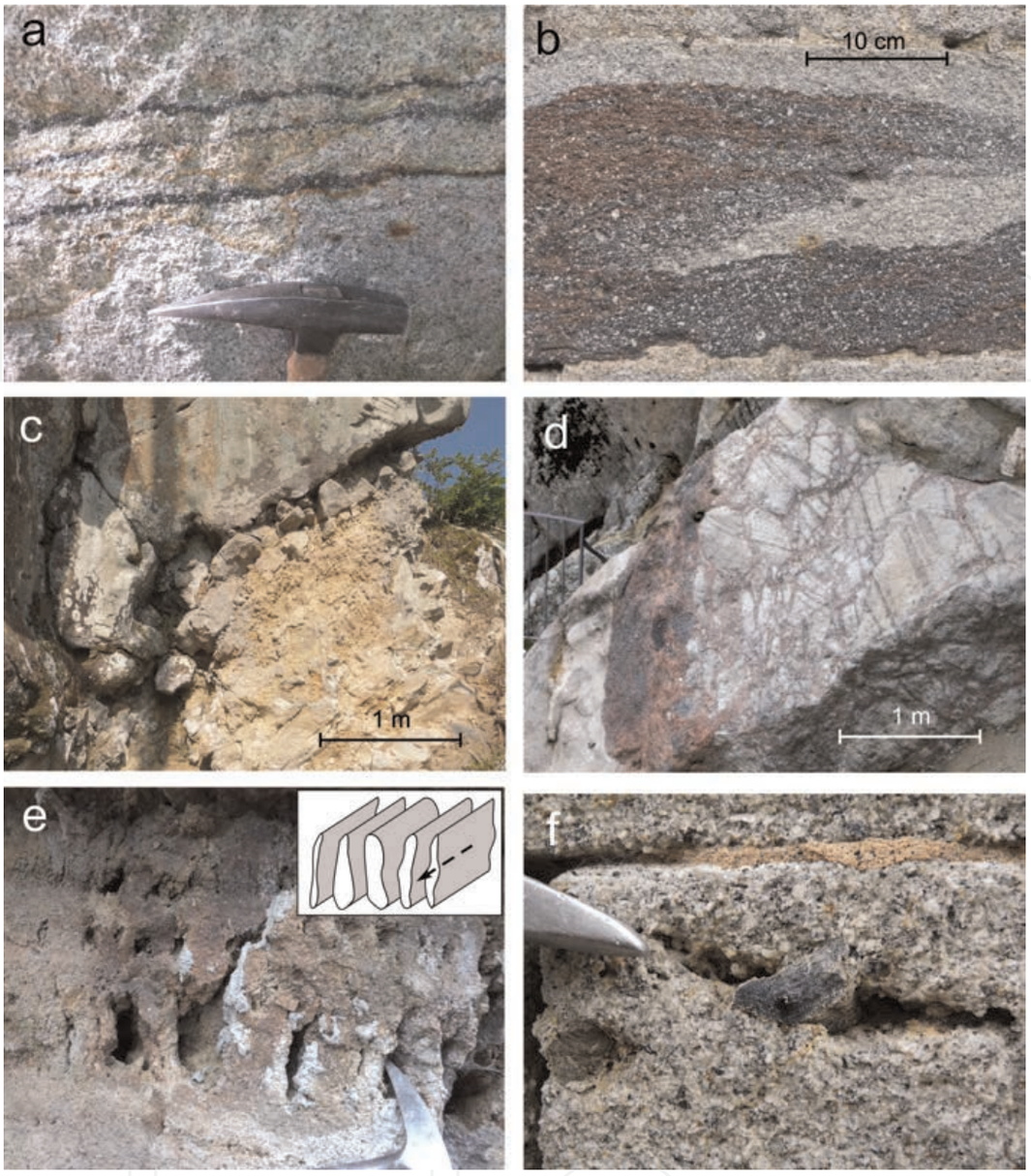

Figure 5.
Outcrop photo of lithofacies and physical volcanological features of the trachydacite SLLFs of Monte Amiata. (a) Bands of black obsidianaceous vitrophyric trachydacite (lithofacies c) in white perlitic vitrophyric trachydacite (lithofacies a; Quaranta unit). (b) Deformed mingling texture between black-to-red obsidianaceous vitrophyric trachydacite (lithofacies c) and white perlitic vitrophyric trachydacite (lithofacies a; Abbadia unit). (c) Basal monogenetic breccia with clastic matrix (lithofacies e) separating two flow units (Piancastagnaio unit). Note the inverse gradation with the larger angular clasts at the top. (d) Interflow monogenetic breccia with laminated trachydacite clasts welded in vitrophyric matrix (lithofacies f; Piancastagnaio unit). (e) Coarse vesicularity with tubular-shaped gas cavities confined in layers (Sorgente del Fiora unit). Inset shows the tridimensional geometry of these cavities that are elongated parallel to the flow direction (arrow). (f) An irregular elongate cavity developed around a meta-sedimentary xenolith (Sorgente del Fiora unit). Hammer for scale where not indicated.

The four coherent lithofacies identified (**Figures 4** and 5; **Table 2**) are as follows: (a) whitish coherent vitrophyric perlitic trachydacite; (b) gray coherent porphyritic microcrystalline trachydacite; (c) black-to-red coherent vitrophyric obsidianaceous trachydacite; and (d) cream-colored coherent vitrophyric microvesiculated trachydacite. Each of these coherent lithofacies shows internal subtle textural variations that include dimensions and abundance in phenocrysts (from fine-grained to coarse-grained porphyricity), vesicles and crystal concentration zones, vesicles layers,

and crystals preferential alignment in fluidal texture. Moreover, lithofacies are arranged in variable vertical and horizontal facies association. At the outcrop scale, the contact between texturally distinct lithofacies is usually sharp.

The three fragmental lithofacies (**Figures 4** and **5**; **Table 2**) are as follows: (e) monogenetic, clast-supported to matrix-supported breccia with fine-grained clastic matrix; (f) monogenetic matrix-supported breccia with clasts welded in a vitrophyric matrix; and (g) monogenetic clast-supported scoria agglomerate. All these fragmental lithofacies have to be considered primary volcanic and autoclastic deposits. In particular:

i. Texture and composition of breccia of lithofacies (e) suggest a formation involving brittle fragmentation at temperatures below the glass transition field [70] of already solidified and flow-laminated lava (**Figures 4** and **5c**).

ii. In lithofacies (f), clast shape and texture suggest that trachydacite was yet rigid at the time of brecciation and that fragmentation occurred *in situ* with scarce disaggregation and transport. Texture and composition of this breccia suggest an initial fracturing and fragmentation at the base of a cooling lava flow unit, followed by its successive welding, as a consequence of the reheating due to the heat advection from the flow to the basal breccia [70, 71]. The overlying coherent trachydacite shows a planar, undeformed flow lamination that parallels the irregular breccia top (**Figure 4f** and **5d**).

4.2.2 Internal structures and textures

Internal structures and textures, such as vesiculation and gas cavities, flow banding, cooling joints, and deformations, have been observed in Monte Amiata SLLFs.

Vesicles and gas cavities are segregation structures of fluids and show different shape, orientation, and dimension in function of their temporal and genetic relationships with the flowing molten lava [72]. In Monte Amiata SLLFs, the dominant coherent lithofacies are poorly or evenly microvesiculated. Vesicles, ranging from less than a millimeter across to cavities more than 10 cm large, are concentrated in trains that form discrete interlayers defining flow layering (**Figure 4e**) and the local flow directions. In coarsely vesicular beds, tubular gas cavities occur together in zones that form planar lenses and layers (**Figure 4e**). The tridimensional geometry of these cavities is complex and unusual (**Figure 5e**). They are apparently continuous for several tens of centimeters in length, horizontally elongated with the main axis parallel to the flow foliation and flow direction. They show an irregular ellipsoidal section, up to 1 cm across and 10 cm along the vertical axis, with scalloped bubble walls (**Figure 5e**). These peculiar gas cavities show some differences as compared with the pipe vesicle typically occurring in basaltic lava [73] that is characterized by individual, subvertical cylindrical tubes with a subcircular section whose formation is attributed to the upward migration of a single bubble of magmatic gas. In the case of Monte Amiata SLLFs, tubular vesicles are formed probably by both the upward coalescence of smaller bubble and lateral migration along the flow direction under the influence of a strong volatile segregation in not-quenched lava. The bubbles confinement in discrete levels may suggest gas entrapment in discrete superimposed domains impermeable among them to the further upward volatile migration. This molten lava partitioning resulted from laminar flow processes, possibly enhanced by the mingling

	Lithofacies	Compositional characteristics	Architecture and occurrence
Coherent lithofacies			
a	Coherent vitrophyric perlitic whitish trachydacite	Massive, evenly porphyritic, equigranular, medium-fine grain (2–5 mm). Groundmass limpid and unaltered glassy, poorly vesiculated, and perlite fractures (2–3 mm). Glomerophyres px + bt + plg; sieved and zoned plg (max 5 cm) and rare K-fs (max 1–2 cm) megacrysts. Poor ME; frequent Msx	Nonuniformly distributed strips and lenses of lithofacies (c). Dominant lithofacies, mainly in Q, C and V units. (**Figure 5a**)
b	Coherent porphyritic microcrystalline gray-to-pink trachydacite	Massive and flow banded, porphyritic, equigranular or seriated, coarse-medium grain. Groundmass microcrystalline—aphyric, locally spherulitic, poorly vesiculated, patches of vesicular pink glass. Glomerophyres plg + bt + px (5–20 mm); sieved and zoned plg (max 5 cm) and rare K-fs (max 1 cm) megacrysts. Abundant ME and Msx.	Interlayer with beds of lithofacies (c) and (d). Well-represented lithofacies, in both flow-banded marginal and frontal parts and massive cores of lava bodies. (**Figure 4g**)
c	Coherent vitrophyric obsidianaceous black-to-red trachydacite	In beds 0.1–10 cm thick, porphyritic, equigranular, medium-fine grain. Groundmass glassy, dense obsidianaceous, not vesiculated, partly perlitic. Glomerophyres plg + bt + px; sieved and zoned plg; rare K-fs (max 1 cm) megacrysts.	Layers and small lenticular patches in lithofacies (a) and (b), planar to very irregular mingling textures [69]. Never outcropping in large individual bodies. (**Figure 5b**)
d	Coherent vitrophyric vesiculated cream-colored trachydacite	In beds 0.1–10 cm thick, poorly porphyritic, medium-fine grain. Groundmass glassy vesiculated, patches of highly vesicular fibrous glass (**Figure 4e**).	Interlayers in the other coherent lithofacies defining a compositional flow lamination. Never outcropping in large individual bodies. (**Figure 4h**)
Fragmental lithofacies			
e	Monogenetic clast- to matrix-supported breccia, fine-grained clastic matrix	Poorly sorted, sometimes inverse-graded. Clasts (cm to dm scale) of blocky, roughly equant, angular to sub-rounded fragments of lithofacies (a) and (b) with flow laminations. Matrix loose to poorly indurated, composed of finer fragments of the same composition.	Thickness 0.5–2 m, lateral extension 1–20 m; after lateral extinction, encasing flow units become para-concordant. Basal breccia in Q and P units, interflow breccia in F and G units, surface breccia in L unit. (**Figures 4** and **5c**)
f	Monogenetic matrix- to clast-supported breccia, clasts welded in a vitrophyric matrix	Poorly sorted. Clasts (cm to dm scale), angular to sub-rounded fragments of lithofacies (a) and (b) with flow laminations, lacking deformation structures. Red and gray coherent vitrophyric matrix welding the clasts, with sharp boundaries; sometimes, matrix is injected in fractures within clasts.	Thickness 0.5–5 m, lateral extension 2–5 m. Clasts' flow lamination evidences little rotation and jigsaw-fit texture. Interflow breccia in F and G units. (**Figure 4f** and **5d**)

	Lithofacies	Compositional characteristics	Architecture and occurrence
g	Monogenetic clast-supported scoria agglomerate	Sub-rounded clasts (dm scale) of coarsely vesiculated, dense fragments (scoriae) of lithofacies (a) and (b). Open framework with scarce and irregularly distributed fine-grained clastic matrix with the same composition of clasts.	Thickness 0.3–1 m, lateral extension limited to few meters. Interflow layer in F and G units.

bt: biotite, K-fs: K-feldspar, plg: plagioclase, px: pyroxene. ME: magmatic enclave, Msx: meta-sedimentary xenolith.

Table 2.
Summary of the macroscopic lithofacies of SLLFs of Monte Amiata trachydacite.

of different lithofacies. Another characteristic of the Monte Amiata SLLFs is the presence of cavities with irregular shape formed around meta-sedimentary xenoliths and megacrysts of plagioclase and sanidine (**Figure 5f**). In this case, gas segregation may result directly from the inclusions.

A layered banded aspect, often flat-lying, is well developed in the Monte Amiata SLLSs, defined both by the interlayering of different lithofacies and by variation in vesicularity, crystallinity, grain size, color, and groundmass texture. Flow bands are laterally continuous, parallel, and dominantly quite planar.

Two types of flow banding must be distinguished in the Monte Amiata SLLFs. A pervasive fine-scale flow banding structure (flow lamination) is produced by interlayering of mm- to cm-sized dark and light laminae of different coherent lithofacies (**Figure 4h**). In addition, sheeting joints, generally attributed to shear partings developed during laminar flow, form well-developed bedding (**Figure 4g**). The stratified structure (flow bedding) comprises massive beds (cm- to m-thick) of porphyritic and vitrophyric coherent lithofacies enclosed at top and bottom by interlayers (mm- to cm-thick) of microvesicular or obsidian lithofacies (**Figure 4a** and **b**). Several processes have been taken into account for the formation of bedding in silicic lavas [74]: (i) mingling of different parts of the magma [75–77]; (ii) welding and rheomorphism [78]; (iii) repeated brecciation followed by reannealing into the conduit [79, 80]; and (iv) laminar flowage inherited during flow in the conduit in response to shear stresses along the conduit walls that continue and propagate upward during the lava advance for the shear stresses at the lava flow base [9].

The flow bands define local sinuosity, steep dips, folding, and convolution in frontal and margin zones of SLLFs (see Section 4.2.3).

Some of the Monte Amiata SLLF trachydacite (Sorgente del Fiora and Piancastagnaio) shows parallel columnar cooling joints that post-date the flow bedding and flow lineation. They are roughly defined, with spacing of 1.5–2.5 m, vary from subvertical to dipping at moderate angles toward the flow front.

4.2.3 Surface and margin structures

At Monte Amiata, *in situ* paleo-weathering, overlaying by younger volcanic units, and current poorly exposure preclude the detection of SLLF original surface structures, such as creases [81] and fractures [82], typical of large silicic lava flows. At the meso-scale, the only surface structures that were preserved in SLLFs include surface ridges or ogives.

Surface ridges or ogives are arcuate reliefs, transversely oriented to the downslope flow. Their convexity indicates the direction of flow. The arcuate shape is caused by the increase in frictional resistance toward the margins of the flow [38, 83]. At Monte Amiata, the presence of surface ridges or ogives is mainly evident on the Quaranta and Castel del Piano units (**Figure 2**). Both these trachydacite SLLFs are stratigraphically below the surface of saprolite paleo-weathering that marks the boundary between BAS and MAS. The Monte Amiata ogives look as linear accumulations of lava boulders. Boulders are rounded-shaped, stacked in an open framework, and arranged in transversal arcuate ridges that are spacing 50–100 m apart from each other with apparent amplitudes averaging 5–15 m upon the topographic surface. These structures have already been distinguished by [30], which, however, considered ogives as the discriminating structure supporting his interpretation of Monte Amiata rheoignimbrites.

Several interpretations have been proposed to explain the formation of ogives on silicic lava flows. Taking Monte Amiata as a model, Rittmann [30] first explained the formation of ogives as pressure ridges due to the differential viscosity between the hot and fluid core and the rigid surface of flows that is compressed and corrugated in folds. The boulders forming the ridges are considered by [30] of primary volcanic origin, resulting as the remnant of rootless dikes of molten material intruded from below in the fractured core of the anticlinal-like ridges subjected to extensive stresses. These seminal ideas of Alfred Rittmann are the premise for various subsequent interpretations. However, most of the observations and models on surface ridges have been addressed to rhyolite obsidian domes and coulées rather than to the structures present on the surface of long silicic lava flows. Macdonald [84] proposed that the ridges on rhyolitic block lava flows are the surface expression of the upward bending—named ramp structure—of the shear planes of the internal flowing lava. The conception that ogives are folds of the lava crust produced by ductile deformation in compression (pressure ridges) as due to differential movements between two layers (center and outside crust of the flow) having temperature and viscosity contrasts was applied by previous scientists [9, 83, 85] among others. Another interpretation proposes that surface ridges are evidence of an extensional regime due to the inflation and deformation of a rigid crust. The moving fluid-rich melt beneath the insulation crust extrudes through regularly spaced cracks forming diapir-like structures [9, 86, 87]. In a more extreme way, Andrews and colleagues [88] challenged the "fold theory" of Fink and proposed that ogives are tensile fracture-bound structures that record brittle failure and stretching of the crust as the lava advances and spreads.

Based on our field observations (**Figure 6**), we interpret the ogives developed on the surface of Monte Amiata SLLFs as compressional structures [89] produced during downslope flowage of viscous silicic lava. The core of these small antiform folds is fractured, enhancing a stronger spheroidal *in situ* weathering of lava in rounded boulders (corestones) during the paleo-weathering processes (**Figure 6**; [62]). Being prominent on the topographic surface, ogives are also the site of more intense surface erosion that removed the sandy saprolite matrix. Consequently, the residual blocks have collapsed in place on themselves forming the boulder accumulations exposed on flow surface [62].

Previous authors [39, 40, 43] have interpreted the surface ridges and boulder accumulations on Monte Amiata SLLFs surface as the evidence of the emplacement of block lava flows. Block lava flows are defined [84, 90, 91] as lava flows in which a highly irregular surface is completely covered by continuous, open clast-supported debris of dense and solidified lava blocks, up to several meters in size, with a

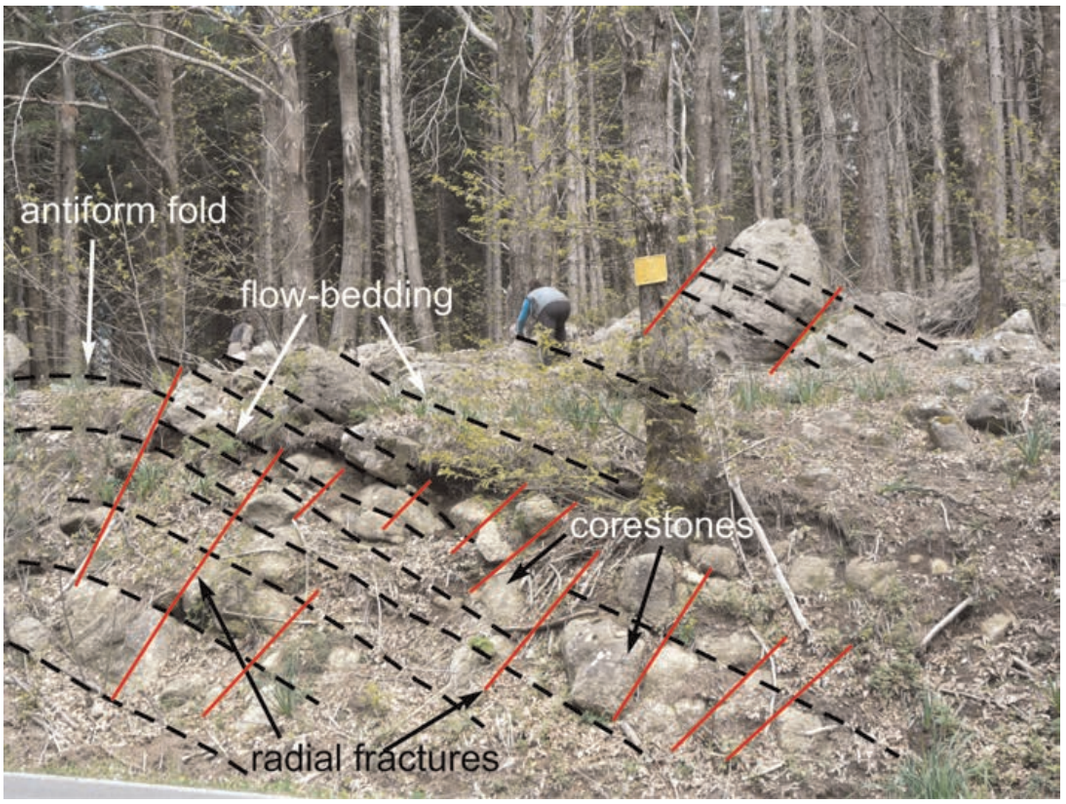

Figure 6.
Natural section showing the internal structure of a ridge (ogive) on the surface of the Quaranta SLLF. The flow banding (dashed black lines) defines an antiform fold. Radially distributed fractures (red solid lines) are related to the extension in the anticline hinge. At the intersection between joints defined by the flow banding and extensional fractures, in situ *saprolite paleo-weathering isolated subrounded corestones of trachydacite. As an extreme effect of this alteration, the ridge resulted as an accumulation of residual lava blocks. Geologist for scale.*

polyhedral shape delimited by smooth, slightly curved faces and angular edges. Normally in the block lava body, a central mass of massive lava is preserved, but the fragmented material remains predominant [84]. Block lavas formed from magmas with silicic to intermediate composition and high viscosity. The mechanism of formation of a blocky breakage of lava is interpreted as dependent on the rapid growth on the flow surface of a thick, more or less glassy crust, which shatters due to the movement of the warmer underlying flow [90]. The extensive deposits of large subrounded lava boulders arranged in arcuate ridges on the surface of the SLLFs of Monte Amiata are not identifiable with the block lava flow as defined above.

The typical structural model of silicic lava flows comprises an internal coherent core enveloped with flow-generated breccia that forms loose deposits on the surface, along the flow margins (levées; [3]) and at the flow front [12]. In Monte Amiata SLLFs, evidence of the presence of lateral levées and accumulation of auto-brecciated debris at the flow front were not observed.

Surface breccia is also absent, but of a localized exception in the Leccio eruptive unit. In the outcrop of Pian di Ballo quarry, located in the medial part of the Leccio lava flow, coherent trachydacite is enveloped with flow-generated breccia (**Figure 7**). Based on texture of the deposit, we distinguished five lithofacies: (1) coherent massive trachydacite with concentric flow foliation forming a monolithic core; (2) coherent stratified trachydacite protruding laterally from the massive core; (3) fractured trachydacite (both massive and stratified) with close fractures and jigsaw cracks; (4)

fragmented and poorly disaggregate trachydacite; and (5) monogenetic, structure-less matrix-supported lithic breccia. These lithofacies undergo lateral transitions with grading boundaries and complex sedimentary architecture (**Figure 7**). Fragmented and poorly disaggregated lava (lithofacies 4) is characterized by polyhedral blocks, up to 1 m large (**Figure 7**) with low intra-clast matrix. Even though most of the blocks are shattered, they retain a recognizable geometry of original bedding and jointing of the

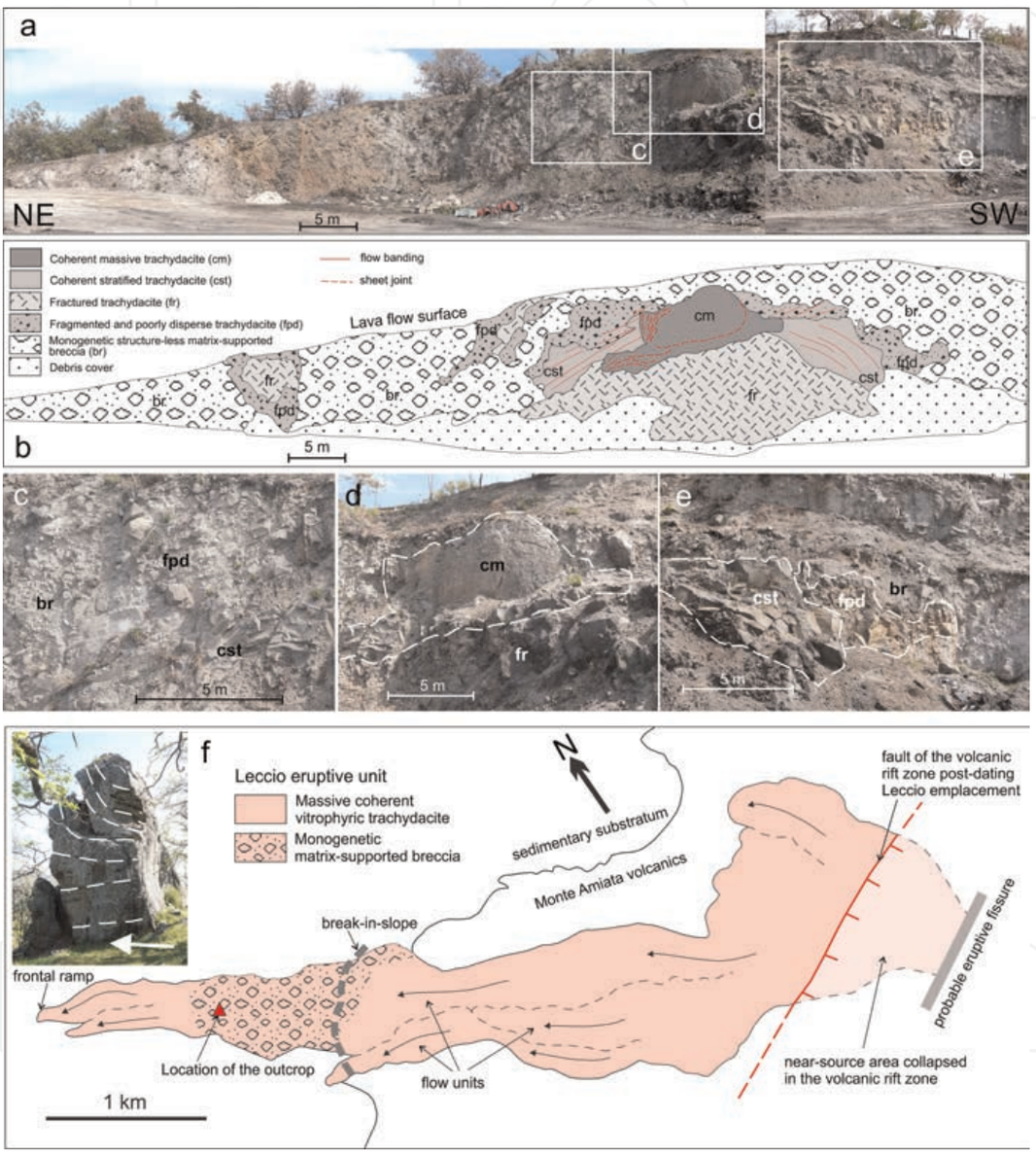

Figure 7.
Quarry escarpment in the locality Pian di Ballo (red triangle in f) showing a complete section transversal to the flow direction of the Leccio SLLF. The structure of the lava flow shows the development of a surface autobreccia. (a) Photo and (b) sketch of the outcrop. A central core of massive trachydacite (cm) with concentric flow foliation is embedded in a monogenetic breccia (br) through progressive fragmentation and dispersion of lava blocks. Although the different lithofacies on the sketch are separated by solid lines, the contacts are gradational. Flow direction is toward the observer. (c) Particular of the gradational transition from coherent trachydacite (cst), to fragmented and poorly dispersed trachydacite (fdp), and to chaotic breccia (br). (d) Close-up of the massive lava core (cm). While the outermost part of the flow was breaking, the center was still molten and moving lava. (e) The flow banded lava (cst) is progressively pervasively fractured by a network of jigsaw cracks but remaining coherent, then is fragmented in a jigsaw-fit breccia that retains the original stratification (fpd), and, finally, is dispersed in the breccia (br). Location of boxes c, d, and e is depicted in a. (f) Map of the Leccio eruptive unit showing the areal distribution of lithofacies and structures. In the inset is the frontal ramp at the edge of the SLLF.

primary depositional and cooling structures of lava flows. Bigger blocks are either fractured or shattered, and many of the block interiors exhibit pervasive jigsaw cracks and jigsaw-fit fractures. This lithofacies represents portions of the coherent pre-fragmentation lavas, slightly disaggregated and displaced. The monolithologic massive and poorly sorted breccia (lithofacies 5) is a chaotic assemblage of matrix-supported clasts from medium to well consolidated. Angular to sub-rounded fragments of trachydacite, ranging from a few centimeters to more than a few decimeters in size, are completely disaggregated and dispersed in the prevailing sandy matrix with the composition of the adjacent clasts. This matrix was likely produced by the disaggregation of the same clasts during transport.

Geologic relationships indicate that fragmentation of a rhyolite lava flow occurred mainly when the flow was spreading [92]. The spatial distribution of the breccia deposit present at the surface of the Leccio eruptive unit (**Figure 7f**) indicates that this unusual (for Monte Amiata SLLFs) volcanic facies probably formed as a function of the change in topography that the lava has encountered during emplacement. From the source area, represented by an eruptive fissure of the summit volcanic rift zone (**Figures 2** and **7f**), the Leccio trachydacite flowed for up to 3 km along a slope of about 15° and then reached a low gradient area (2–3° in slope) without confining walls at the edge of the volcanic edifice. When the flow arrived at the abrupt break-in-slope, it decelerated, and a dynamic block fragmentation occurred at the margins and surface of the flow, forming the monogenetic matrix-supported breccia observed in this part of the Leccio eruptive unit (**Figure 7**). The increase in the degree of fragmentation suggested by the textural characteristics of the breccia (grain size reduction, jigsaw cracks, and jigsaw-fit fragmentation), proceeding from the internal coherent core to external surfaces of flow, is probably the consequence of progressive fracturation, disaggregation, and dilation processes that have occurred during this deceleration phase [93, 94]. Then, the massive coherent trachydacite core (**Figure 7d**) resulted in a thermally insulated internal part of the lava that continued to flow downstream confined through a paleo-valley, attaining a total length of more than 6 km (**Table 1**), and terminated with a frontal ramp structure (**Figure 7f**).

Monte Amiata SLLFs have steep flow front, tens of meters thick, exhibiting ramp structures and monoclinal folds outlined by the orientation of the flow bedding (**Figure 8**). In ramp structures, the flow bedding varies from a flat foliation parallel to the base of the flow to an upward curved, steeply dipping to vertical shape. The stack of layers involved in the upward spoon-shaped deformation overrides along a plane of shearing and discontinuity the underlying gently dipping layers (**Figure 8a**). Contact occurs without the interposition of breccia. Moving upstream away from the ramp, the attitude of the flow bedding becomes para-concordant. These ramp structures have been observed near the frontal portion of several flow units and are probably to be attributed to an increased stress regime owing to an increasing frictional resistance toward the base of the flow ramp. Indeed, they are well developed at the front of flow that was channelized and ponded in paleo-valleys (Leccio and Vivo d'Orcia; **Figure 7f**, **8a** and **b**). The ramp structures observed in Monte Amiata SLLFs are different from both the sheet-like flow ramps described in obsidian block lava flows and attribute to individual flow units having upper and lower surfaces that are composed of *in situ* brecciated, brittle glassy carapaces (i.e., the Rocche Rosse flow at Lipari; [95]) and ramps triggered by shear planes inside the lava interior and related to the formation of surficial ogive structures [96].

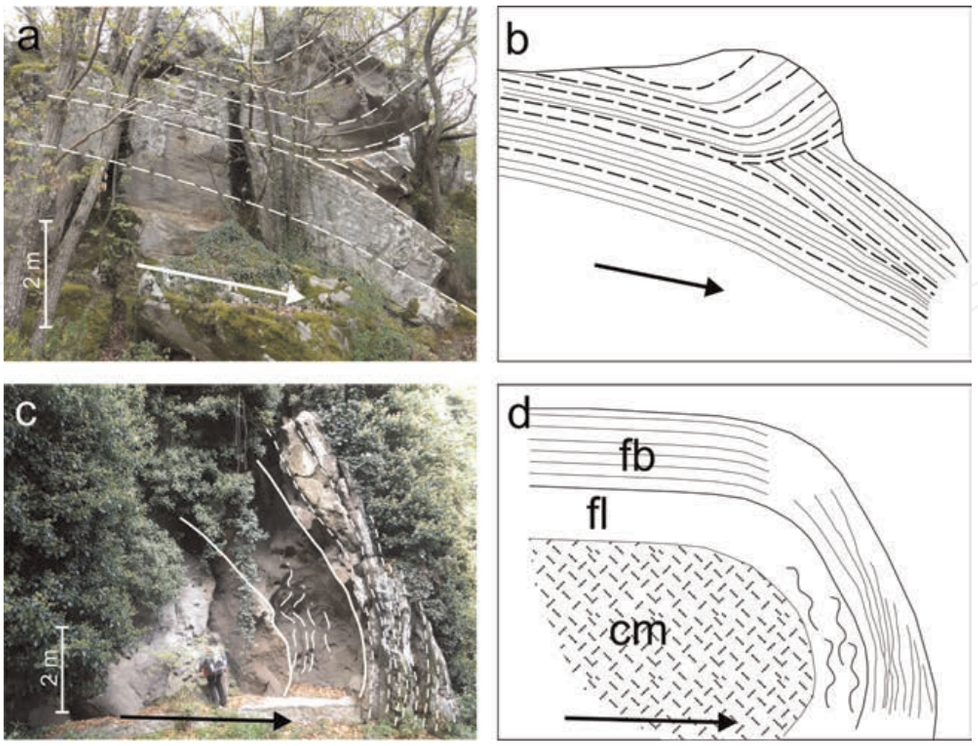

Figure 8.
Flow front structures in SLLFs of Monte Amiata. (a) Outcrop exposure and (b) interpretative sketch of flow ramp structure at the flow front of Vivo d'Orcia eruptive unit composed of fine laminated vitrophyric trachydacite with perlitic glassy groundmass. Arrow is the flow direction. Note the transition from para-concordant to discordant bedding and the absence of breccia deposits. (c) Outcrop exposure and (d) interpretative sketch of monoclinal fold structure of the flow front of Piancastagnaio eruptive unit. The core of the fold is composed of coherent massive trachydacite (cm), enveloped in flow-laminated (fl) and flow-banded (fb) trachydacite. Along the subvertical limb of the fold, the flow-laminated lava is deformed in small asymmetric parasitic folds and the flow-banded lava is stretched.

Another type of flow front observed at Monte Amiata consists of layers which, instead of being bent upward, as in the ramps, are bent downward to form a monoclinal fold (**Figure 8c** and **d**). In this case, flow bedding is planar and sub-horizontal in the upper part of the flow body, whereas near the front, it curves sharply downward until it becomes subvertical. Flow bedding experienced a stratal stretching and thinning caused by the extension in the fold limb (**Figure 8c** and **d**). The core of the fold is composed of coherent massive trachydacite, enveloped by faintly tiny laminated trachydacite with layers deformed in crumpled minor folds. Locally, a detachment surface has been observed at the base of the frontal fold. Also in this case, the deformation occurs without the presence of breccia. This type of flow front has been observed in the Piancastagnaio and Sorgente del Fiora eruptive units.

Flow front of lavas usually is obscured by a talus apron. At Monte Amiata, the presence of frontal breccia has never been observed. It cannot be excluded *a priori* that breccia has been completely removed by erosion, but the lack of both any deposit remains and its continuation in a basal breccia lead to the interpretation of an emplacement mechanism different from that of rhyolite lava flows.

4.3 Facies architecture

Within a single flow unit, the vertical and lateral lithofacies distribution and association allows to recognize a characteristic structural partitioning of lava flow interior [11, 97]: (i) basal zone; (ii) core or central zone; and (iii) upper zone.

i. The basal zone [12, 98] of BAS SLLFs typically rests directly on the surface of the underlying unit (sedimentary substratum or older volcanic units in core drill DL) without intervening pyroclastic, volcaniclastic, sedimentary, or pedogenetic layers. MAS SLLFs overlay the paleo-weathering saprolite deposit developed at the expense of BAS units. The SLLF basal zone is generally 2–5 m thick and comprises a breccia bed (lithofacies e; **Table 2**) or a shear zone (**Figure 9**). The occurrences of basal breccia are localized; the contact between the basal breccia and the overlying lava is typically sharp. In the classic models [12, 99], basal breccia is interpreted as originated as crumble breccia at the surface of slowly moving masses of lava, which concurs to form the steep flow front talus and then was overridden as the lava advanced. In Monte Amiata SLLFs, both the absence of surface and frontal breccia deposits and the texture of the basal breccia observed suggest that the basal breccia is produced *in situ* by shear fragmentation. In most cases, the basal breccia is lacking, and the bottom of SLLF is composed of bedded facies with flow layering of glassy and microcrystalline trachydacite (lithofacies a, b, and d; **Table 2**), planar or tightly folded, and sparse—greatly stretched—shrinkage gas cavities.

ii. The central (lava core) zone [12] in SLLFs of Monte Amiata is typically 20–40 m thick and comprises massive and bedded facies, with joints and flow

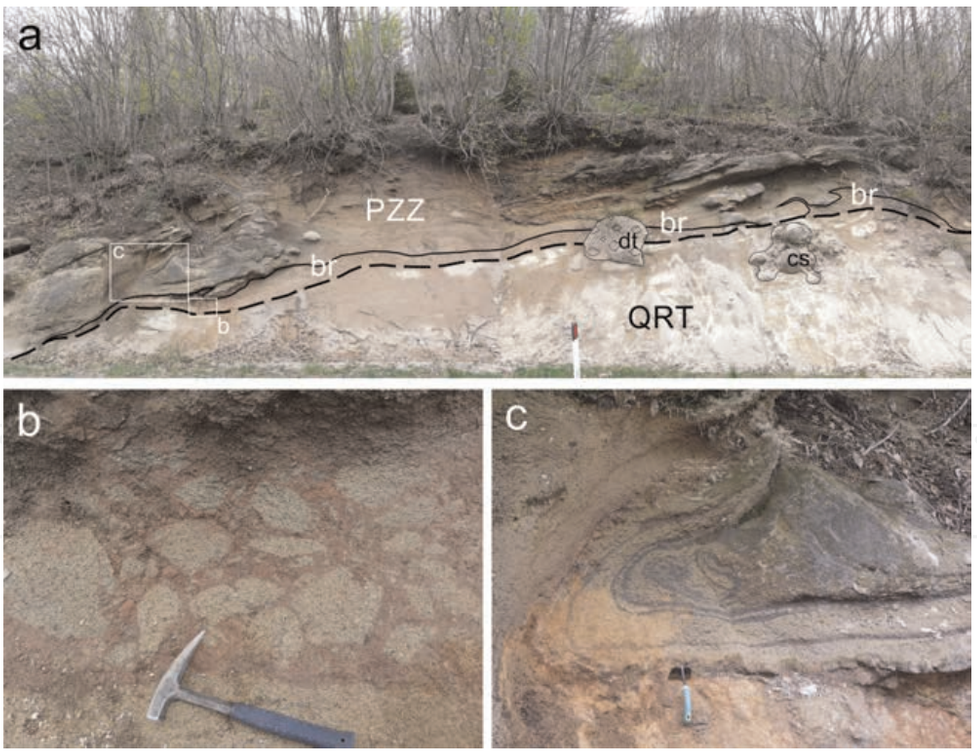

Figure 9.
(a) Overview of the outcrop showing the contact between the Quaranta (QRT) and Pozzaroni (PZZ) SLLFs. The upper portion of the Quaranta lava flow (BAS-MSS) has been in situ *paleo-weathered into a whitish sandy saprolite with groups of corestones (CS). The basal zone of the Pozzaroni lava flow is composed of a discontinuous bed of monogenetic matrix-supported breccia (br) overlaid by flow-bedded trachydacite. Both breccia and stratified basal trachydacite are deformed in convoluted folds. dt =debris. Boxes refer to b and c details. (b) Close-up of the breccia at the base of PZZ eruptive unit. The flow lamination in the clasts is randomly oriented. (c) Detail of the recumbent fold and convoluted structures at the base of PZZ formed during the flow for the high viscosity of the lava.*

layering. Massive lava is generally uniform and dense. Lava shows poorly developed, vertical, or locally inclined columnar joints a few to several meters across (i.e., Sorgente del Fiora and Piancastagnaio eruptive units). Subhorizontal sheeting joints are also present and are more conspicuous near the top and base of the central zone. Flow layering is parallel to aligned crystals and vesicle-rich layers and is interpreted as planes of weakness imparted by the flowage. In some units (i.e., Sorgente del Fiora and Vivo d'Orcia eruptive units), lenses and irregular zones of welded breccia (lithofacies f; **Table 2**) and scoriaceous agglomerate (lithofacies g; **Table 2**), with an individual thickness of 0.5–1.5 m, form interlayers between otherwise massive lava banks. We interpret that these interlayers resulted from intra-flow fragmentation processes within a single eruptive unit, probably related to stresses caused by movement in the overlying flow.

iii. The upper zone of Monte Amiata SLLFs trachydacite is characterized by a moderately more vesicular groundmass and a planar morphology forming subhorizontal plateaus and poorly inclined sides. It does not show the typical structure of lithophysae, strong vesiculation, and scoriaceous or blocky autobreccia classically described for the top of large silicic lava flows [12, 92]. The absence of these surface structures is confirmed by the stratigraphic log of the Sorgente del Fiora unit in the DL core (**Figure 4**), even if it cannot be excluded that in other units, they were present but currently poorly exposed or subsequently eroded.

4.4 Geochemical and petrographic characteristics

The whole chemical composition of the lava flows (LF) and domes (LD) at Monte Amiata ranges from latite to trachydacite (SiO_2 = 57–68 wt%; $Na_2O + K_2O$ = 7–9 wt%; **Figure 10**) [40, 42, 44, 57, 58, 100]. In variable proportion through the entire sequence, millimetric to pluri-decimetric in size, meta-sedimentary xenoliths and microgranular magmatic enclaves (ME) are present. The ME compositions range from trachybasalt to latite (SiO_2 = 47–59 wt%; $Na_2O + K_2O$ = 5–8 wt%; **Figure 10**; [58]). A careful selection (**Table 3**) of data from literature shows that all the SLLF samples are among the most evolved rocks of the suite and classify them as trachydacite (SiO_2 = 64–68 wt%; $Na_2O + K_2O$ = 8–9 wt%; **Figure 10**) having a normative q > 20% (q = Q/(Q + or + ab + an)*100) [101].

The SLLFs are highly porphyritic (about 40% according to [41]), medium- to coarse-grained, with maximum dimensions of the phenocrysts rarely exceeding 1 cm (**Table 4**). The most abundant phenocrysts are plagioclase, K-feldspar, orthopyroxene, and biotite, and less abundant are apatite, ilmenite, and quartz, rarely present clinopyroxene (**Table 4**). The presence of fragmented crystals is peculiar, especially of K-feldspar (**Figure 11a** and **b**). Content in mafic magmatic enclaves is scarce, while tabular meta-sedimentary xenoliths are more frequent.

Instead, the lava domes, coulées, and short lava flows are medium to high porphyritic ranging from 26 to 34% [41, 56], with similar mineral paragenesis, but are characterized by the distinctive presence of K-feldspar megacrysts (from 1 to 5–6 cm long) coupled with abundant microgranular magmatic enclaves [40, 42, 44, 57].

The SLLFs are generally porphyritic to glomeroporphyritic with a glassy groundmass commonly showing perlitic fractures. Different groundmass microtextures are observed, also in the same unit: (i) glassy groundmass microlite-free (**Figure 11c**) or

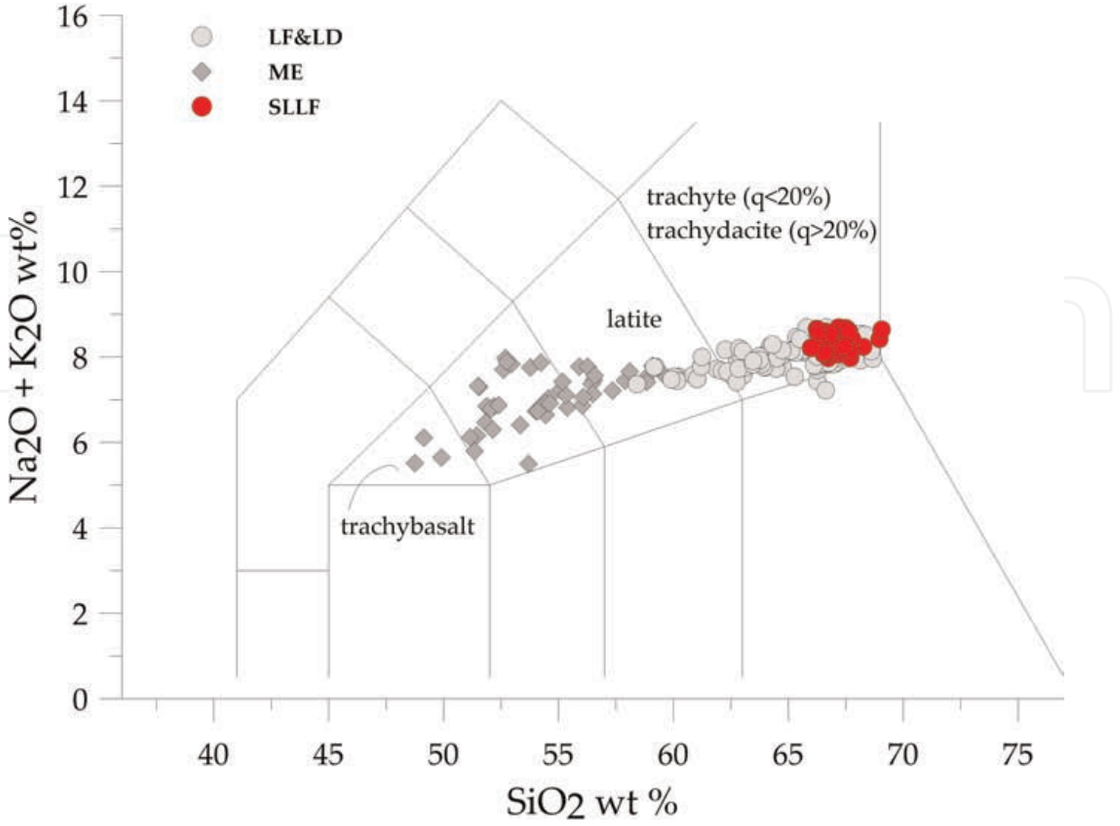

Figure 10.
*T.A.S. (Total Alkali-Silica) diagram for products of Monte Amiata volcano: Silicic lava flows and lava domes (LF + LD; light gray dots), magmatic enclaves (ME; dark gray diamonds), and SLLF units studied in this work (red dots; **Table 2**). Data from [39–42, 44, 57].*

(ii) with ultra-microlites aligned to the flow direction (**Figure 11d**); (iii) glassy groundmass locally devitrified with scattered spherulites (**Figure 11e**); and (iv) heterogeneous groundmass with flow banding in elongated bands or lenses generally of a darker color (**Figure 11f**). Flow bands are normally enriched in crystal fragments (**Figure 11g**); (v) highly vesicular with fibrous glass and large flattened vesicles (**Figure 11h**).

4.5 Temperature, pressure, and dissolved volatile content in Monte Amiata magmas

In order to retrieve the conditions (i.e., pressure, P; temperature, T; and volatile content) of magma in the storage system and during the dynamics of ascent toward the surface, and to understand eruption dynamics of Monte Amiata SLLF generating magmas, we have applied the numerous geothermobarometers and geohygrometers so far available in the literature, accounting for both "crystal," "crystal-crystal," and "crystal-residual liquid" equilibria. The compositions of the lavas for which calculations were performed are reported in **Table 3**. More details about the contour conditions (e.g., mineral-liquid duplets; preliminary estimations by independent variables; necessary equilibrium tests) necessary to apply each specific model are reported in [102].

The list of geothermobarometers and hygrometers adopted is reported in **Table 5** [103–107], together with the temperature interval of application of magma ascent and

Label	SLLF[1]	Ref [2]	SiO_2 wt%	TiO_2	Al_2O_3	$Fe_2O_3^*$	FeO	MnO	MgO	CaO	Na_2O	K_2O	P_2O_5	LOI	Sum
84 BB	A	3	64.67	0.52	16.30	3.19		0.04	1.53	2.75	2.03	5.70	0.18	2.97	99.88
AMT 47	A	2, 4	66.28	0.52	16.33	1.11	2.00	0.05	1.23	2.75	2.14	6.16	0.18	1.26	100.00
AMT 48	A	2, 4	65.69	0.52	16.67	0.38	2.72	0.05	1.27	2.71	2.12	5.99	0.17	1.72	100.00
AMT 94	A	4	67.43	0.49	16.27	0.59	2.26	0.04	1.31	2.13	2.17	5.97	0.13	1.22	100.00
AMT 17–145	A	5	64.30	0.51	15.70	3.46		0.05	1.36	2.72	2.26	6.04	0.16	1.85	98.52
84 AV	C	3	65.89	0.49	16.08	3.67		0.05	1.28	3.02	2.21	5.74	0.16	1.28	99.87
AM 11	C	1	66.57	0.52	15.90	2.06	1.38	0.05	1.43	3.01	2.26	5.73	0.20	0.87	99.98
AM 13	C	1	66.11	0.50	15.70	2.07	0.91	2.41	0.05	2.53	2.13	5.90	0.19	1.51	100.01
AM 19	C	1	66.98	0.54	16.05	2.56	0.59	0.05	1.33	2.76	1.96	5.93	0.18	1.06	99.99
AMT 06	C	2, 4	65.82	0.59	16.36	0.61	2.72	0.06	1.19	2.96	2.20	6.06	0.18	1.26	100.00
AMT 08	C	4	66.25	0.56	15.52	0.83	2.48	0.06	1.21	2.97	2.22	6.35	0.15	1.40	100.00
AMT 09	C	4	66.81	0.51	15.63	0.85	2.20	0.05	1.13	2.95	2.28	6.23	0.15	1.22	100.00
Amt 10	C	2, 4	66.40	0.53	15.70	0.72	2.52	0.06	1.32	2.99	2.37	5.91	0.16	1.25	99.93
AMT 10	C	2, 4	66.73	0.56	15.54	0.60	2.52	0.05	1.19	2.96	2.28	6.29	0.17	1.12	100.00
AM 37	F	1	68.27	0.48	15.26	2.14	0.64	0.05	1.11	2.56	2.20	6.14	0.15	1.01	100.01
AMT 50	F	4	65.74	0.58	15.80	0.48	2.76	0.05	1.36	3.16	2.14	6.04	0.16	1.74	100.00
AMT 51	F	2, 4	65.70	0.54	16.06	0.43	2.76	0.05	1.33	2.98	2.13	5.95	0.16	1.91	100.00
84 BD	G	3	65.42	0.47	16.22	3.69		0.05	1.28	3.11	2.19	5.74	0.15	1.56	99.88
AMT 56	G	2, 4	66.90	0.50	15.64	0.16	2.80	0.05	1.27	2.93	2.18	6.14	0.15	1.28	100.00
AM 16	L	3	68.34	0.48	15.19	2.41	0.36	0.05	1.13	2.30	2.30	6.25	0.15	1.20	100.16
AMT 01	L	2, 4	66.91	0.58	15.51	0.50	2.56	0.05	1.19	3.00	2.25	6.24	0.16	1.05	100.00
AMT 03	L	2, 4	66.14	0.62	15.83	0.49	2.76	0.06	1.27	3.20	2.23	6.09	0.18	1.14	100.00
AMT 04	L	2, 4	66.01	0.56	15.87	0.77	2.68	0.06	1.28	3.08	2.18	6.11	0.16	1.25	100.00

Label	SLLF[1]	Ref [2]	SiO_2 wt%	TiO_2	Al_2O_3	$Fe_2O_3^*$	FeO	MnO	MgO	CaO	Na_2O	K_2O	P_2O_5	LOI	Sum
AMT 13–10	L	5	65.70	0.51	16.10	3.66		0.06	1.41	3.00	2.40	6.19	0.17	1.41	100.73
AMT 13–21	P	5	66.00	0.55	16.00	3.74		0.06	1.40	2.39	2.17	6.26	0.17	1.58	100.42
AM 71	Q	3	66.87	0.51	15.95	2.18	0.97	0.05	1.29	2.72	2.40	5.63	0.18	1.25	100.00
AMT 60	Q	2, 4	65.36	0.63	16.36	0.53	2.76	0.06	1.34	2.87	2.29	6.22	0.17	1.41	100.00
AMT 14–57	Q	5	66.00	0.54	15.90	3.74		0.06	1.45	3.20	2.39	6.10	0.18	1.51	101.17
84 AZ	V	3	65.01	0.50	16.62	3.85		0.06	1.43	2.80	2.16	5.93	0.17	1.72	100.25
84 BA	V	3	65.60	0.50	16.03	3.75		0.05	1.45	3.21	2.21	5.93	0.16	0.98	99.87
AMT 96	V	4	65.22	0.51	17.55	1.23	1.72	0.04	1.30	2.31	2.17	5.75	0.17	2.04	100.00
AMT 97	V	2, 4	66.60	0.50	16.12	1.75	1.64	0.04	1.21	2.61	2.18	5.95	0.15	1.25	100.00
AMT 95	V	2, 4	64.81	0.55	17.47	0.19	2.84	0.05	1.44	2.54	2.16	5.90	0.19	1.86	100.00

[1]Label of SLLF units as in ***Figure 2****: A. Abbadia, C. Castel del Piano, F. Fiora, G. Piancastagnaio, L. Leccio, P. Pozzaroni, Q. Quaranta, V. Vivo D'Orcia).[2]References: 1: [58], 2: [40], 3: [42], 4: [44], 5: [57].* *Total iron as Fe_2O_3.*

Table 3.
Representative chemical whole rock compositions of selected samples of SLLF from Monte Amiata.

Groundmass texture	Glassy with perlitic fractures, subordinate aphanitic, and devitrified in spherulites (unit P); variable amount and distribution of vesiculation, stretched and folded vesicles aligned according to flow foliation (units F, P, Q, and V), sometimes filled by secondary precipitation minerals (e.g. cristobalite) (unit P); variable amount (few to abundant) of microlites and spider- and needle-shaped ultra-microlites (mainly K-fs and px) aligned according to flow foliation
Phenocrysts assemblage[1]	K-fs (medium 5 mm, rare up to 1.5 cm); plg (3–5 mm); opx (2–3 mm); bt (medium 1–3 mm, abundant, euhedral and up to 4 mm in units A, P, Q, and V); rare cpx (unit F); glomeroporphyres of plg + opx + bt units F, G, Q, and V)
Mineral phases and microstructures[1]	K-fs: mainly fragments of larger crystals, Carlsbad twinning (unit F), rounded and lobate rims; some poikilitic texture including melts and crystals (plg, bt and crystal aggregate of plg + opx) (units A, L, Q, and V) Plg: complex zoned crystals with sieve-textured and patchy-zoned resorbed nucleii (highly altered into alluminosilicate minerals e.g., allophane) and oscillatory-zoned rims., often host fluid, glass and mineral inclusions(e.g., bt, opx, Fe-Ti oxides), commonly as crystal cluster (C, F, G, P, and V) Bt: abundant, sometimes opacized; folded, broken in thin lamellae, and containing sub-spherical holes (sieve texture) and mineral inclusions Opx: deep embayments and rounded opacized rims include small euhedral apatite and Fe-Ti oxides. Cpx: rare, in microphenocrysts and microlites Fe-Ti oxides: microphenocrysts: commonly included in other minerals Quartz: abundant highly resorbed crystals (unit L)
ME/xenoliths	Holocrystalline aggregates (plg + opx + bt), abundant in units P and Q Meta-sedimentary xenoliths, dark gray, platy, fine-grained, composed of: (i) green spinel+bt + feldspar, unit A, (ii) green spinel + graphite, with a feldspar corona, and "baked clay"-like fragments, unit L, (iii) green spinel + quartz + cordierite with plg + bt corona, unit Q, and iv) aggregates of acicular crystals bt/phlogopite + plg + K-fs + cpx + glass, unit V

[1]Mineral phases: K-fs = K-feldspar; plg = plagioclase; cpx = clinopyroxene; opx = orthopyroxene; bt = biotite. ME: mafic magmatic enclave. Labels of SLLF units as in ***Figure 2****.*

Table 4.
Microscopic petrographic characteristics of Monte Amiata SLLFs.

lava flow dynamics. Our results all show that the lavas emitted at Monte Amiata represent, in terms of temperature, an extreme end member for each of the compositions and mineral assemblages investigated here.

On the basis of the results provided in **Table 5**, we can distinguish two sample subsets: (1) a first group (PES, preeruptive stage) characterized by crystalline liquid balances associated with a phase of initial crystallization, where the liquid is the total rock, representative of a preeruptive or initial phase of ascent; (2) a second group (ES, eruptive stage) where the liquid phase in equilibrium with a specific crystalline phase is the interstitial fluid. This group has been related to a late phase of the crystallization occurred during the ascent of the magma and/or during the mass emplacement of lavas. The PES group shows temperature estimates between 900°C and 1070°C, whereas ES group has temperature range between 800°C and 900°C. These temperature ranges constitute the entire temperature interval provided by the employment of all the geothermometers analyzed and constitute therefore an enlarged estimate of the real intervals of expected temperature.

The estimation of dissolved water content (hereafter reported as H_2O and expressed in wt%) is of fundamental importance to comprehend the storage and

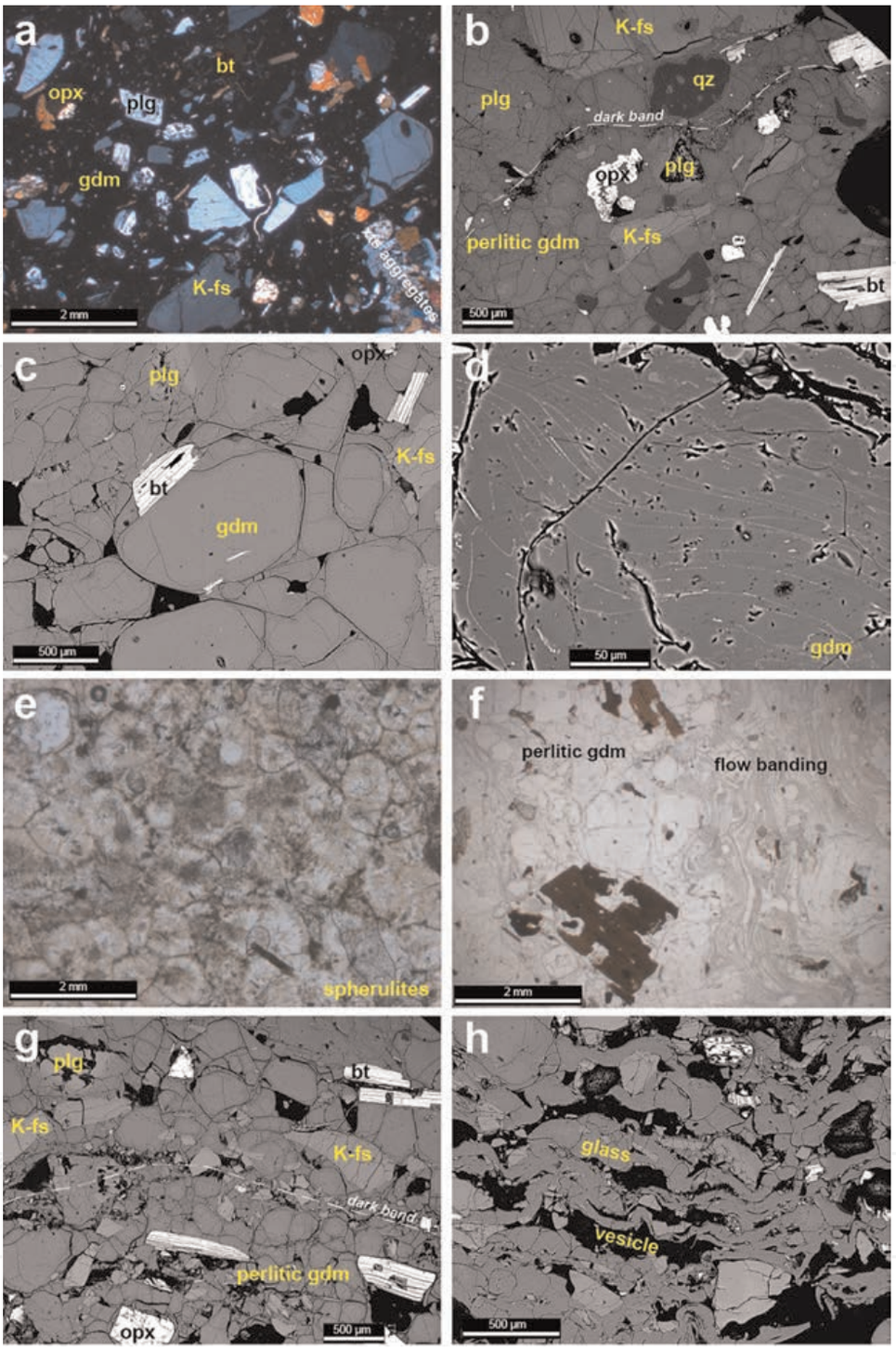

Figure 11.
(a) Highly porphyritic texture: The phenocrysts are fragmented crystals of K-feldspar, plagioclase, orthopyroxene, biotite set in a glassy groundmass (optical microscopic image crossed polarized, unit Q, sample AMT 14–51); (b) broken crystals of K-feldspar, zoned plagioclase, orthopyroxene, biotite, and resorbed quartz set in a perlitic glassy groundmass (BSE-SEM image, unit L, sample AMT 14–71b); (c) glassy groundmass, microlite-free, with perlitic texture (BSE-SEM image, unit L, sample AMT 13–10b); (d) glassy groundmass with ultra-microlites (probably Fe-Ti oxides) aligned to the flow direction (BSE-SEM image, unit L, sample AMT 13–10b); (e) devitrified groundmass with spherulites (optical microscopic image plane polarized, unit P, sample AMT 14–54); (f) heterogeneous glassy groundmass with perlitic texture and darker flow bands (optical microscopic image plane polarized, unit L, sample AMT 14-71b); (g) glassy groundmass with perlitic texture and flow band enriched in crystal fragments (BSE-SEM image, unit L, sample AMT 13–10); (h) highly vesicular glassy groundmass with large flattened vesicles (BSE-SEM image, unit L, sample AMT 13–10). Labels of SLLFs as in ***Figure 2****. bt: biotite; gdm: groundmass; K-fs: K-feldspar; opx: orthopyroxene; plg: plagioclase; qz: quartz, xts: crystals.*

	Plg-liquid			Cpx-liquid				Apatite
*	Eq. 23	Eq. 24a	Eq. 26	Talk1	Talk2	Talk3	Talk4	
Unit								
				Total rock (TR)				
SLLF	(1030–1050)	(993–1015)	(965–993)	980	(955–998)	965	(914–1014)	(905–940)
				Glass matrix (GM)				
SLLF	(877–888)	(824–838)	(832–845)	—	—	—	—	(879–883)

Temperature calculated by using ([103, 104]; Eqs. 23, 24a, 26) plagioclase model for only the Plg-liquid couples which passed equilibrium test (2.2.1.). GM and TR are the groundmass liquids and the total rock liquids, respectively. Talk1, Talk2, Talk3, and Talk4 are the temperature intervals calculated for each Cpx-liquid equilibrium combination which passed the equilibrium tests. Temperature values referred to as Talk1, Talk2, Talk3, and Talk4 correspond to the re-calibration of [105] models of [106]. The apatite geothermometer, reported as apatite, is the value calculated for the [104] geothermometer. More details can be found in [102]. A temperature interval between 900°C and 1070°C is assumed to be ideal for the initial crystallization at depth, whereas a lower temperature interval (800°C and 900°C) is likely characteristic of the late crystallization condition at the shallow levels, emplacement, or post-emplacement.
**Reported equations are as from [103, 104].*

Table 5.
Summary of the minimum and maximum temperature values estimated by using the geothermometers proposed by [102] for the SLLF of the BAS and MAS.

ascent conditions of magma, as well as the eruption style and emplacement of the volcanic products. H_2O, in fact, more than any other component, affects the physical properties of the magmatic and volcanic materials as well as the associated processes (diffusivity, crystallization, and degassing). One weight percent of H_2O dissolved in a SiO_2-rich magma may change its viscosity of ca. 6 orders of magnitude and its glass transition temperature (i.e., the temperature at which, upon certain stress conditions, there a transition between a viscous to a brittle mechanical behavior occurs) of 200°C.

Since there are no data on the CO_2 concentration of melt inclusions, the H_2O-CO_2 saturation model of [108] (https://melts.ofm-research.org/CORBA_CTserver/GG-H2O-CO2.html) was used to estimate the fluid content of the magma stored in the Monte Amiata magma chamber positioned at 6 km depth [49, 109, 110], where the expected external pressure is 106 MPa and temperature is 900–1070°C (see before). The average oxide percentage was considered (**Table 3**) in calculations. The H_2O and CO_2 mole fractions in the fluid phase were varied to compute the H_2O and CO_2 in the coexisting melt at 900–950°C, whereas no results were obtained at higher temperatures. Outcomes are reported in **Figure 12**, showing that maximum H_2O concentration is 3.96–3.98 wt% for zero CO_2 and maximum CO_2 concentration is ca. 500 ppm for zero H_2O.

Of course, the H_2O and CO_2 concentrations in the deep magma might be everywhere along these lines. Nevertheless, it must be recalled that in the Monte Amiata edifice and surrounding area, a strong degassing of magmatic/mantellic CO_2 occurs as indicated by high CO_2 fluxes from soil [111, 112], the presence of CO_2 in the fluid inclusions [113], and the composition of geothermal fluids ([114]; and references therein).

Therefore, owing to this occurrence of magmatic/mantellic CO_2, the magma in the Monte Amiata chamber might be saturated with CO_2 and consequently water concentration would be low or even very low, although this possibility is a hypothesis to be proven or rejected by means of melt inclusions data. If this hypothesis is true, CO_2 would be readily lost upon degassing and H_2O concentration would weakly decrease, thus explaining the lack of explosive activity at Monte Amiata.

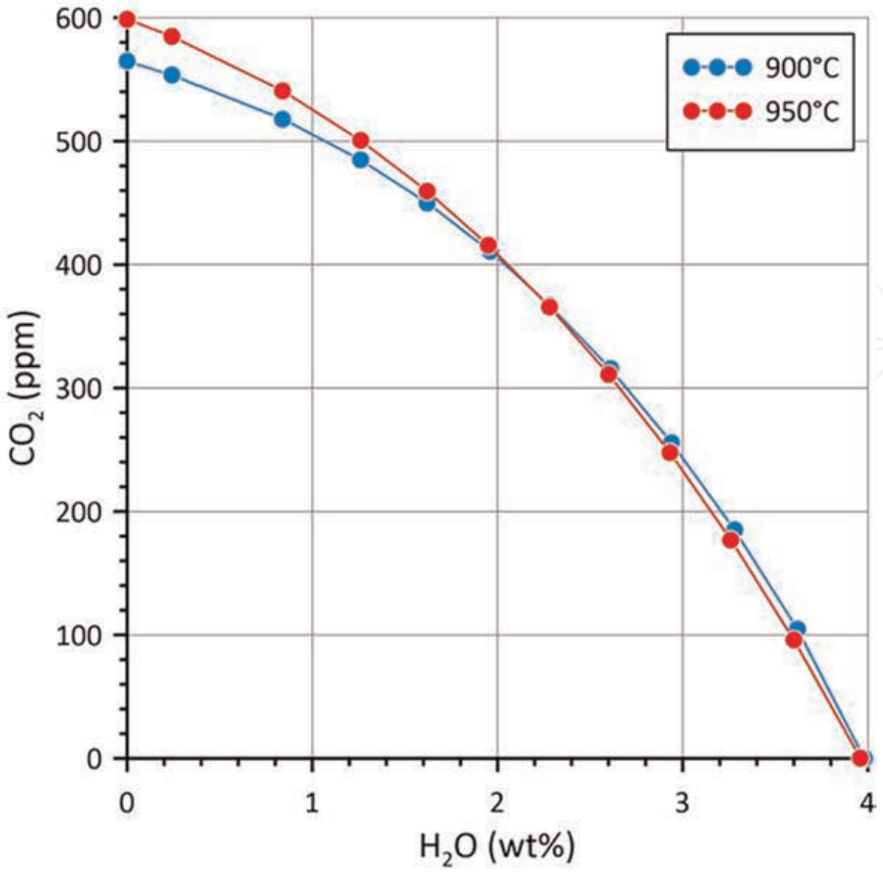

Figure 12.
CO_2 vs. H_2O coexistence in melt calculated by means of the saturation model of [108] for temperature of 900°C (blue line and dots) and 950°C (red line and dots).

4.6 Rheological properties

In order to quantify the effect of rheology on Monte Amiata eruptive style, in this study we combine two empirical models. The first model (GRD) [115] allows to calculate the residual liquid viscosity as a function of the temperature (T) and the composition (X). The second model (CM) [116] allows to estimate the rheological effects due to the presence of crystals in strained magmas, through the calculation of the relative viscosity (i.e., the ratio between the viscosity of the mixture and the viscosity of the pure liquid). The input data are constituted by the textural data providing the crystal fraction (Section 4.4), the temperature estimation, and dissolved fluid content (Section 4.5).

Figure 13 reports the pure liquid viscosity vs. the inverse of the temperature. The calculations are performed on the entire temperature range, but we put in evidence the interval 900–1070°C, representative of an early-stage-crystallization (PES) magma and the interval 800–900°C, representative of the late-stage-crystallization magma and erupted products (ES). Considering the total content of fluids present inside this magma, which is strongly influenced by the presence of CO2—see Section 4.5—and considering that the latter is completely separated from the magma during the ascent and the emplacement process, a quantitative of 0.3 wt% of residual water appears acceptable as an input parameter into the proposed models. The crystal fraction of the suspended crystals presents in each SLLF is based on the average values proposed by [41]. These values are reported in

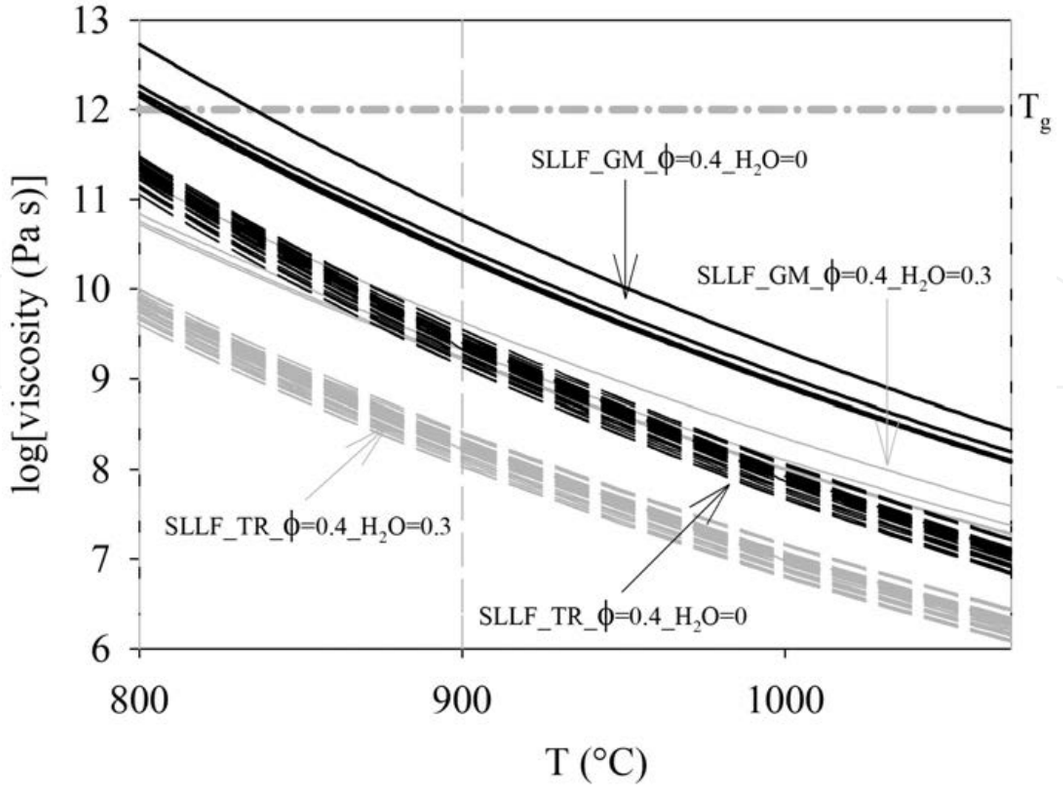

Figure 13.
Diagram of the calculated liquid + crystal suspension viscosity values for the investigated Monte Amiata SLLFs. Here, the suspending liquid is taken as the residual glass matrix (GM) or as the total rock (TR), whereas the crystal content (ϕ) is taken as the value proposed by [45] of 40 volume % (ϕ=0.4). Water content (H_2O) is considered to be 0 or 0.3 wt% as potentially presence as dissolved at the basis of the most tick lava flows. The calculations provided here do not account for the effect of suspended vesicles in the multiphase magmatic and volcanic mixture. For that reason, we could assume that the calculated values are an upper limit of the real volcanic mixture viscosity (vesicles in fact have an important effect in reducing magmatic and volcanic mixture viscosity), which may be representative of the most glassy crystal rich (vesicle free) lavas as those found at Monte Amiata. The figure also reports (at 10^{12}Pa s, in dash and dot thick gray) the line which marks the glass transition, that is, at first approximation, representative of the limit of viscous flow of lava flows [70]. In all cases, the calculated volcanic mixture viscosities estimated in the temperature interval (900–1070°C) are well below the flow limit as above defined. Both GM and TR, at any crystal and water content conditions in the (800–900°C) temperature interval, mostly fall below Tg and, only at the very lowest T, they overpass it.

volume percent (the number in the parenthesis followed by the symbol %). All the calculations are carried out by assuming the lowest strain rate value (10^{-5} s^{-1}), which provides the highest viscosity value.

In **Figure 13,** we also report the value of the glass transition temperature (Tg) as taken at a viscosity of 10^{12} Pa s [70]. Tg constitutes that barrier below which most of processes (e.g., diffusion, crystallization, vesiculation, flow, and welding) are significantly inhibited, if not halted. On the other hand, above the glass transition, the above-mentioned processes are still active and potentially rapid enough to still influence somehow the magmatic and volcanic processes. Ref. [117] published a comprehensive review of the ways how the various magmas and volcanic bodies may cross the glass transition temperature (e.g., conventional thermal cooling; cooling along a retrograde solubility curve; effective raising of Tg as due to degassing) and enhance the welding of pyroclastic materials or the flow of silicic lavas, other than affecting the depth of the fragmentation depth.

5. Discussion

5.1 Distinguishing silicic lavas from welded tuffs and rheomorphic ignimbrites

Several scholars have attempted to compare and define diagnostic textures and structures to explain how silicic lava flows differ from high-temperature pyroclastic density currents (welded and/or rheomorphic ignimbrites) (e.g., [11, 15, 71, 99]). In this section, we discuss the geological and volcanological features (field physical features and rock's textures and structures) that support the interpretation of trachydacite sheet-like silicic flows of Monte Amiata as lavas and reject the attribution as welded ignimbrites and rheoignimbrites deriving from the emplacement of pyroclastic density currents emitted during a single large explosive eruption.

In **Table 6,** we summarize (i) the diagnostic depositional characteristics of ignimbrite [1, 118–120] that have not found in Monte Amiata trachydacite SLLFs despite careful search, and (ii) the discriminating internal textures and structures of the Monte Amiata trachydacite SLLFs that help to identify them as silicic lava flows [12, 121–123].

In conclusion, the volcanological observations, the field geological evidence, and the petrographic analyses performed on the trachydacite SLLFs of Monte Amiata are consistent with a genetic interpretation by effusive eruptions, which gave rise to long and extensive silicic lava flows.

5.2 Defining a model of silicic lava flows (SLLFs) for Monte Amiata trachydacite

Observations and models on silicic lava flows have been mainly carried out on small rhyolite obsidian domes and coulées [9, 87, 89] that have some characteristics that were extended to other silicic lavas. The idealized structural model of rhyolite lava flow [92] consists of three principal zone: (1) a basal pyroclastic deposit emplaced during the initial phase of the eruption, (2) a lava dome or short flow formed by the relatively quiet effusion of magma, and (3) an envelope of carapace breccia that grows around the molten core of the lava body as the chilled and brittle outer crust breaks in response to internal expansion and growth. The lava body is further subdivided in a vertical sequence of: basal part composed of breccia of pumice and obsidian blocks, interior part composed of either coarsely vesicular pumice, coherent even flow-foliated glassy obsidian, and finely vesicular pumice, and surface breccia [89].

More recently, a certain number of studies have been carried out so far it concerns the emplacement mechanisms of very large lava flow sequences in the Brazilian sector of the early Cretaceous Paranà Etendeka Magmatic Province (PEMP) [19–21]. Apparently, these huge effusive silicic sequences (> thousands of km^3) were not accompanied by explosive activity. The same authors have invoked mechanisms, which explain the emplacement of the investigated lava flows as mainly due to the emission of degassed dacitic and rhyolitic low-viscosity lavas.

The peculiarity of Monte Amiata sheet-like trachydacite lava flows appear to have some point in common with those found in the products reported in the PEMP and, with respect to other described silicic flows, their main features, without considering the greater length of the SLLF, are as follows:

a. Absence of tephra or air-fall pumice deposits testifying explosive activity associated with the lava emplacement. Commonly, sequence of explosive

Textural discriminating characteristics	Diagnostic value
Features distinguishing SLLFs from ignimbrite	
Fragmentary vitroclastic textures (bubble-wall shards, small pumice fragments, fiamme) none observed.	Even in the very densely welded ignimbrites occurrences of shards and pumice are generally anyway recorded.
Evidence of welding not observed.	Also in strongly welded tuffs, some remains of welding textures are preserved due to vertical and lateral gradation from completely non-welded to fully welded facies.
Lithofacies do not record gradational changes in texture and structure from near source to distal areas of flow.	Adjacent to vent, ignimbrites show only particulate flow facies varying from vitrophyric welded tuffs and polygenetic lithic-rich breccia, and grade to massive pumice-and-ash flows, and finally to mass flows completely managed by gravity (lahars, debris flow) [118–120].
Vertical and lateral association of facies, derived from different eruptive and emplacement mechanisms, but still generated by the same explosive eruptive event, not observed.	Basal Plinian fallout, co-ignimbrite ash fallout, and low-density pyroclastic flows can be present in the basal, intermediate, and top parts of the ignimbrite deposit.
Features indicative of effusive style of emplacement	
Coherent texture with high content in phenocrysts (40 vol%, [41]) in a homogenous transparent vitrophyric or microcrystalline groundmass.	Texture indicating crystallization from a non-particulate melt.
Very little vertical and lateral variation in mineral paragenesis and chemical composition, within individual trachydacite flows.	Textures indicating crystallization from a non-particulate melt.
Fluidal texture due to well-developed crystals lineation and elongated vesicles, preservation of delicate-textured glomerocrysts.	Textures indicating effusion and spreading of lava; in ignimbrites, the prominent development of foliation is by flattening of pumice fragments during welding.
Flow-layered structures due to banding (color, lithofacies, and vesicularity), and parting along flow planes.	Structures suggesting laminar flow of coherent lava; layering is favored by shear near the base of the flow.
Folding of flow bands, mainly at the flow front and margins.	Suggests high viscosity of a non-particulate melt.
Small to large-scale mingling domains of obsidian glassy, microcrystalline, and vesicular glassy coherent lithofacies, in bands and lenses [75].	Textures indicating emplacement from a non-particulate melt. In an explosive event, magma mingling textures are destroyed by disruption of the magma and exhibited only in discrete pyroclasts.
Small content (<10%) in broken crystals.	The presence of low percentages of broken crystals is therefore characteristic of silicic viscous lavas and is interpreted as the response to shear stress during laminar flow [121].
Lithic inclusions of mafic magmatic enclaves and meta-sedimentary xenoliths of basement units that were at a deep of about 6 km in the upper crust, where the magmatic chamber formed [109, 122].	In ignimbrites, lithic fragments derived from the disaggregation of the wall rocks by shallow explosion [123] (near vent) or incorporation from the ground during flowage (near base).
Basal and internal monolithologic autoclastic breccia, composed of coarse scoria clasts or blocky co-genetic lithic clasts in a sandy matrix with the same composition as clasts.	Indicative of lava-like viscous flow rather than particulate flow.

Textural discriminating characteristics	Diagnostic value
Step flow front a few tens of meters thick with ramp structures; and marginal flow lobes [12].	Indicative of lava-like viscous flow that suddenly stopped; ignimbrite shows gradual thinning at edges of unit.
Arcuate ogives on flow surface.	Formed as folds while the lava was in motion; viscosity decreases downward from the surface to the interior of the flow.
Well-defined areal distribution of individual flows, also in a relatively flat topography; several flows ponded in paleo-valleys.	An ignimbrite would have inundated the flanks of the volcano and climbed over many barriers.

Table 6.
Characteristics of Monte Amiata SLLFs supporting the interpretation as lava flows.

eruptions of tephra preceding (and/or following) the extrusion of silicic lava flows and domes is observed [89, 124]. In similar cases, the early-stage explosive activity was considered functional to gas escape from magma and to the subsequent effusive activity.

b. Absence of talus debris commonly mantling the steep front, margins (levées), and surface (upper breccia) of silicic lava flows and domes and originating by syn-eruptive rockfall of highly disrupted surficial portions of lava. This implies that we cannot apply to Monte Amiata SLLFs the interpretation that the basal breccia derived by the fracturing of the cooler, finely vesicular, pumiceous crust during lava movement that fall off at the front and are overridden by the advancing lava, forming a nearly continuous envelope around the more viscous flow interior [89].

c. Some SLLFs show several lobe outflows (i.e., Pozzaroni; **Figure 2**) deriving from the breakout of the lava front and margins, similar to basaltic lavas. This process extended the lava field and suggests that the thick lavas are maintained, even for a long time, substantially above the glass transition temperature, representative of the temperature of flow halting [70], favoring their mobility and the run-out of long distances [5, 6, 102].

d. A high porphyricity in a glassy fresh groundmass that is commonly not devitrified and lacking of spherulitic texture, whereas most described silicic lavas show aphyric or non-porphyritic glassy (obsidian or pumiceous) texture.

e. Absence of a quenched or highly vesicular crust.

f. No correlation is observed between area and slope values, suggesting that the different areal distribution of SLLFs can be substantially independent from the underlying morphology.

The recognition of large-volume, extensive silicic lava flow units at Monte Amiata introduces questions regarding the mechanisms of emplacement. Into the literature, the uncommon sheet-like silicic lava flows are related to the effect of large erupted volume and the effectively lava heat retained due to a thick solidified

crust, whereas the dome-forming eruptions of silicic lavas are related to low-magma production rates [125].

Thanks to the direct observation of the events of silicic lava flow emplacement occurred in historical time [2–7], we have understood that the emplacement of large volume and great thickness silicic lava flows with high proportions of suspended crystals should not surprise us.

In fact, it has demonstrated by [5, 6, 126] and, more recently, [19, 20], that the large thickness of a lava flow constitutes the most efficient thermal barrier, which reduces heat loss and allows to maintain the lavas at high temperature well above their glass transition temperatures. This will favor, for years, or even for decades, in the cases of the largest fluxes, the flow. To favor flow will favor other important processes, such as the crystallization of the spherulitae and the contribution of the volatile resorption [117, 127].

In conclusion, the unusual length and the main characteristics described above (absence of related tephra deposits, absence of talus debris, presence of outflow lobes, high porphyricity, glassy fresh groundmass, and absence of quenched or highly vesicular crust) of the SLLFs of Monte Amiata may be referred to the high temperature, high thicknesses, and relatively large volume of each one of these lava flows. In this picture, morphological factors and volatile content seem to have played a minor role.

5.3 Volcano-tectonic and structural implication into the silicic volcanism of Monte Amiata

At Monte Amiata, the association of silicic volcanism with transtensive shear zones [45, 55] was significant in determining the volcanological character of the silicic volcanism. In this work, we were able to define the near-vent features, buried under younger units, and to infer the source area on the basis of thickness, physical features, and distribution of Monte Amiata SLLF eruptive units. The vent area of SLLFs was possibly identified with an eruptive fissure system located near the crest of the summit ridge and fed by linear dike swarms (**Figure 2**). A multi-vent source is recorded by changes in location of eruption source (**Figure 2**).

Monte Amiata magmas were vented by faults related to regional transtension along the Bagnore-Bagni San Filippo shear zone that has been active during the volcano activity [45, 55], leading to dominantly effusive eruptions.

Referring to this structural framework, the SLLFs of Monte Amiata are put in place following the ascent along a system of faults which in their upper portion define a summit axial rift zone, rather than real volcanic conduits. The geometry of these upwellings and the reduced quantity of gas present in the magma are probably the main factors that inhibit the formation of a fragmentation surface [45]. While the ability of this lava flows to maintain their viscosity, their anomalously high temperature for a long time determines the style of emplacement in long and thick lava flows.

6. Conclusions and future researches

The outstanding questions on Monte Amiata sheet-like trachydacite that we discuss in this work are mainly related to the interpretation of its eruption mechanisms (effusive vs. explosive volcanism) that we have faced with an unprecedented physical and volcanological characterization of the products and by comparing our results with the updated models of ignimbrite and rheoignimbrite. The identification of several

lava flow eruptive units (referring to different eruptive events and vents location) having different stratigraphic position and composed of several flow units separated by scoria or breccia beds is the first argument for this discussion. The second main discussion point is the manner of flowing of single lava flows and the reasons for producing the different volcanic facies and structures we observed and described. Our results point out to a model for the formation of the Monte Amiata SLLFs which could possibly be extended to other silicic composite volcanoes.

In major detail, our field-based study of the trachydacite SLLFs of Monte Amiata supports these conclusions:

1. The volcanic deposits of Monte Amiata, both outcropping and present in the subsoil of the volcano, recently crossed by deep drilling, are exclusively made up of a set of silicic lava flows, lava domes, and associated coulées.

2. The SLLFs include different individual effusive eruptive units that are well recognizable from each other and well traceable on the field. They have different stratigraphic position in the volcanic succession that prevents to consider all these lavas as coeval and/or emitted in a single episode of magmatic feeding and eruption.

3. The arcuate ridges of trachydacite boulders present on the surface of SLLFs are to be referred to pervasive phenomena of *in situ* paleo-weathering of lavas at the expense of surficial fold structures (ogives).

4. The repeated presence of SLLFs at different levels of the stratigraphic volcanic sequence implies that, during the geological history of the volcano, there have been conditions for a recurrence of an eruptive mechanism emplacing long and extensive silicic lava flows. This peculiar behavior of a silicic magma can possibly be attributed to the ascent along eruptive fractures of batches of magma with low gas content and anomalously high temperatures. These physicochemical conditions enabled lavas to flow slowly but inexorably up to the distances granted to them by the internal thermal balance. For this reason, the lavas morphologically forced by valley incisions flow at major distances in proportion to the others that flow unconfined (**Table 1**), because the greater thickness and the smaller exchange surface with the soil and the atmosphere allow a greater conservation of the temperature inside them. This temperature surplus could be originally due to a higher value of the ratio between the temperature times the volume of the melt still residing in the magma chamber and the temperature times the volume of the more basic magma coming from the deep.

5. The tectonic control on the feeding system has meant that the magma supply was managed by the activity of the various deep and superficial fracturing trends. This type of control is able to create the conditions to inhibit the formation of a fragmentation surface and generate an entire volcano through a succession of exquisitely fissural eruptions in a regime of volcano-tectonic rift.

Looking to the future, the data still missing on Monte Amiata products are represented by the quantification of the volatile content in magmas, and by the definition of the silicic-magma/mafic-magma ratio characterizing the feeding of the single events. Obtaining these further pieces of information will allow us to further

refine the model presented here for the formation of SLLFs and, in a broader perspective, the model of the other lithofacies (lava domes and coulées) that have been emplaced during the various phases of the life of the completely silicic Monte Amiata volcano.

Acknowledgements

This work has been initially funded by the Regione Toscana (Italy) by means of the LAMMA Consortium in the framework of the project of a volcanological monograph of Monte Amiata edited at the end of 2017, and then by JRC-EPOS project. Prof. Luigi Marini is acknowledged for the fruitful discussion on fluid fraction inside Monte Amiata magmas. SLF is grateful to T. Abebe Adhana for priceless help in optical microscope observations.

Author details

Luigina Vezzoli[1,2*], Claudia Principe[2], Daniele Giordano[2,3,4], Sonia La Felice[2] and Patrizia Landi[2,5]

1 Science and High Technology Department, Insubria University, Como, Italy

2 Institute of Geosciences and Earth Resources, National Research Council, Pisa, Italy

3 Earth Sciences Department, Torino University, Torino, Italy

4 Institute of Sciences and Technologies for Ceramic Materials, National Research Council, Faenza, RA, Italy

5 National Institute of Geophysics and Volcanology, Pisa Section, Pisa, Italy

*Address all correspondence to: luigina.vezzoli@gmail.com

IntechOpen

References

[1] Branney MJ, Kokelaar P. Pyroclastic density currents and the sedimentation of ignimbrites. Geological Society Memoir. 2002;**27**:1-143

[2] Navarro-Ochoa C, Gavilanes-Ruíz JC, Cotés-Cortés A. Movement and emplacement of lava flows at Volcán de Colima, México: November 1998–February 1999. Journal of Volcanology and Geothermal Research. 2002;**117**:155-167

[3] Harris AJL, Flynn LP, Matias O, Rose WI, Cornejo J. The evolution of an active silicic lava flow field: An ETM+ perspective. Journal of Volcanology and Geothermal Research. 2004;**135**:147-168

[4] Pallister JS, Diefenbach AK, Burton WC, Muñoz J, Griswold JP, Lara LE, et al. The Chaitén rhyolite lava dome: Eruption sequence, lava dome volumes, rapid effusion rates and source of the rhyolite magma. Andean Geology. 2013;**40**:277-294. DOI: 10.5027/andgeoV40n2-a06

[5] Tuffen H, James MR, Castro JM, Schipper CI. Exceptional mobility of an advancing rhyolitic obsidian flow at cordon Caulle volcano in Chile. Nature Communications. 2013;**4**:2709. DOI: 10.1038/ncomms3709

[6] Farquharson JI, James MR, Tuffen H. Examining rhyolite lava flow dynamics through photo-based 3D reconstructions of the 2011–2012 lava flow field at Cordón-Caulle, Chile. Journal of Volcanology and Geothermal Research. 2015;**304**:336-348

[7] Magnall N, James MR, Tuffen H, Vye-Brown C. Emplacing a cooling-limited rhyolite lava flow: Similarities with basaltic lava flows. Frontiers Earth Science. 2017;**5**:44. DOI: 10.3389/feart.2017.00044

[8] Fink JH, Anderson SW. Emplacement of Holocene silicic lava flows and domes at Newberry, South Sister, and Medicine Lake Volcanoes, California and Oregon. U.S. Geological Survey, Scientific Investigations. Report. 2017;**5022**(I)

[9] Fink JH. Structure and emplacement of a rhyolite obsidian flow: Little Glass Mountain, Medicine Lake Highland, northern California. Geological Society of America Bulletin. 1983;**94**:362-380

[10] de Silva SL, Self S, Francis PW, Drake RE, Ramirez CR. Effusive silicic volcanism in the Central Andes: The chao dacite and other young lavas of the Altiplano-Puna volcanic complex. Journal of Geophysical Research. 1994; **99**:17805-17825

[11] Gibbon DL. Origin and development of the Star Mountain Rhyolite. Bulletin of Volcanology. 1969;**33**:438-474

[12] Bonnichsen B, Kauffman DF. Physical features of rhyolite lava flows in the Snake River Plain Volcanic Province, southwestern Idaho. Geological Society of America Special Paper. 1987;**212**: 119-145

[13] Henry CD, Price JG, Rubin JN, Laubach SE. Case study of an extensive silicic lava: The Bracks rhyolite, trans-Pecos Texas. Journal of Volcanology and Geothermal Research. 1990;**43**:113-132

[14] Henry CD, Wolff JA. Distinguishing strongly rheomorphic tuffs from extensive silicic lavas. Bulletin of Volcanology. 1992;**54**:171-186

[15] Manley CR. Physical volcanology of a voluminous rhyolite lava flow: The Badlands lava, Owyhee plateau, southwestern Idaho. Journal of

Volcanology and Geothermal Research. 1996;**71**:129-153

[16] Allen SR, McPhie J. The Eucarro rhyolite, Gawler range volcanics, South Australia: A 675 km^3 compositionally zoned felsic lava of Mesoproterozoic age. Geological Society of America Bulletin. 2002;**114**:1592-1609

[17] Allen SR, Simpson CJ, McPhie J, Daly SJ. Stratigraphy, distribution and geochemistry of widespread felsic volcanic units in the Mesoproterozoic Gawler Range Volcanics, South Australia. Australian Journal of Earth Science. 2003;**50**:97-112

[18] Loewen MW, Bindeman IN, Melnik OE. Eruption mechanisms and short duration of large rhyolitic lava flows of Yellowstone. Earth Planetary Science Letters. 2017;**458**:80-91

[19] Polo LA, Giordano D, Janasi V, Freitas-Guiaraes L. Effusive silicic volcanism in in the Paraná Magmatic Province, South Brazil: Physico-chemical conditions of storage and eruption and considerations on the rheological behaviour during emplacement. Journal of Volcanology and Geothermal Research. 2018;**355**:115-135

[20] Polo LA, Janasi V, Giordano D, Canon Tapia E, Lima E, Roverato M. Effusive silicic volcanism in the Paraná Magmatic Province, South Brazil: Evidence for local fed lava flows and domes from detailed field work. Journal of Volcanology and Geothermal Research. 2018;**355**:204-218

[21] Giordano D, Vona A, Gonzalez-Garcia D, Allabar A, Kolzenburg S, Polo LA, et al. Viscosity of Palmas-type magmas of the Paraná Magmatic Province (Rio Grande do Sul State, Brazil): Role on eruption dynamics of high-temperature silicic volcanism. Chemical Geology. 2021;**560**:119981

[22] Agangi A, Kamenetsky VS, McPhie J. Evolution and emplacement of high fluorine rhyolites in the Mesoproterozoic Gawler silicic large igneous province, South Australia. Precambrian Research. 2012;**208-211**:124-144

[23] Besser ML, Gouvea Vasconcellos EM, Ranalli Nardy AJ. Morphology and stratigraphy of Serra Geral silicic lava flows in the northern segment of the Torres trough, Paraná Igneous Province. Brazilian Journal of Geology. 2018;**48**:201-219

[24] Leggett TN, Befus KS, Kenderes SM. Rhyolite lava emplacement dynamics inferred from surface morphology. Journal of Volcanology and Geothermal Research. 2020;**395**:106850. DOI: 10.1016/j.jvolgeores.2020;106850

[25] Ayalew D, Pyle D, Ferguson D. Effusive Badi Silicic Volcano (Central Afar, Ethiopian Rift); Sparse Evidence for Pyroclastic Rocks. In: Németh K, editor. Updates in Volcanology. London, UK: Intechopen; 2021. p. 16. DOI: 10.5772/intechopen.98558

[26] Peccerillo A. The Tuscany Province. In: Peccerillo A, editor. Cenozoic Volcanism in the Tyrrhenian Sea Region. 2nd ed. Cham: Springer International Publishing AG; 2017. pp. 19-60

[27] Vezzoli L, Principe C. Monte Amiata volcano (Tuscany, Italy) in the history of volcanology: 1—Its role in the debates on extinct volcanoes, source of magma, and eruptive mechanisms (AD 1733-1935). Earth Science History. 2020;**39**:28-63

[28] Sabatini V. Analogie tra Monte Amiata e Monte Cimino. Atti Reale Accademia Lincei Rendiconti. 1910;**5-19**: 284-290

[29] Sabatini V. Lave che sembrano tufi e tufi che sembrano lave. Bollettino Società Geologica Italiana. 1911;**30**: 913-921

[30] Rittmann A. Cenni sulle colate di ignimbriti. Bollettino Accademia Gioenia Scienze Naturali di Catania. 1958;**4-10**: 524-533

[31] Rutten MG. Acid lava flow structure, as compared to ignimbrites. Bulletin Volcanologique. 1963;**25**:111-121

[32] Wolff JA, Wright JV. Rheomorphism of welded tuffs. Journal of Volcanology and Geothermal Research. 1981;**10**:13-34

[33] Principe C, Vezzoli L. Monte Amiata volcano (Tuscany, Italy) in the history of volcanology: 2—Its role in the definition of "ignimbrite" concepts and in the development of the "rheoignimbrite" model of Alfred Rittmann. Rendiconti Accademia dei Lincei Scienze Fisiche e Naturali. 2020;**31**:539-561

[34] White DA. Report on the International Association of Volcanology (IAV) Symposium on Ignimbrites and Hyaloclastites, Italy, 1 September-1 October 1961. Commonwealth of Australia, Department of National Development, Bureau of Mineral Resources Geology and Geophysics, Records. 1962;**101**:1-44

[35] Andrews GDM, Branney MJ. Emplacement and rheomorphic deformation of a large, lava-like rhyolitic ignimbrite: Grey's landing, southern Idaho. Geological Society of America Bulletin. 2011;**123**:725-743

[36] Brown DJ, Bell BR. The emplacement of a large, chemically zoned, rheomorphic, lava-like ignimbrite: The Sgurr of Eigg pitchstone, NW Scotland. Journal of the Geological Society. 2013;**170**:753-767

[37] Marinelli G. Genesi e classificazione delle vulcaniti recenti toscane. Atti Società Toscana di Scienze Naturali in Pisa, Memorie Serie A. 1961;**68**:63-116

[38] Rittmann A. Volcanoes and their Activity. New York-London: Interscience Wiley; 1962

[39] Mazzuoli R, Pratesi M. Rilevamento e studio chimico petrografico delle rocce vulcaniche del Monte Amiata. Atti Società Toscana di Scienze Naturali in Pisa, Memorie Serie A. 1963;**70**:355-429

[40] Ferrari L, Conticelli S, Burlamacchi L, Manetti P. Volcanological evolution of the Monte Amiata southern Tuscany: New geological and petrochemical data. Acta Vulcanologica. 1996;**8**:41-56

[41] Cristiani C, Mazzuoli R. Monte Amiata volcanic products and their inclusions. Periodico di Mineralogia. 2003;**72**:169-181

[42] Cadoux A, Pinti DL. Hybrid character and pre-eruptive events of Mt. Amiata volcano (Italy) inferred from geochronological, petro-geochemical and isotopic data. Journal of Volcanology and Geothermal Research. 2009;**179**: 169-190

[43] Marroni M, Moratti G, Costantini A, Conticelli S, Benvenuti MG, Pandolfi L, et al. Geology of the Monte Amiata region, Southern Tuscany, Central Italy. Italian Journal of Geosciences. 2015;**134**: 171-199

[44] Conticelli S, Boari E, Burlamacchi L, Cifelli F, Moscardi F, Laurenzi MA, et al. Geochemistry and Sr-Nd-Pb isotopes of Monte Amiata volcano, Central Italy: Evidence for magma mixing between high-K calc-alkaline and leucititic mantle-derived magmas. Italian Journal of Geosciences. 2015;**134**:268-292

[45] Vezzoli L, Principe C. Building a completely effusive silicic composite volcano: Geologic history, architecture, and volcanic-tectonic interactions of Monte Amiata (Middle Pleistocene, Italy). Submitted to. Journal of Volcanology and Geothermal Research. 2022

[46] Scrocca D, Doglioni C, Innocenti F. Constraints for an interpretation of the Italian geodynamics: A review. Memorie Descrittive della Carta Geologica d'Italia. 2003;**62**:15-46

[47] Molli G. Northern Apennine Corsica orogenic system: An updated overview. Geological Society of London Special Publication. 2003;**298**:413-442

[48] Calcagnile G, Panza G. The main characteristics of the lithosphere-asthenosphere system in Italy and surrounding regions. Pure and Applied Geophysics. 1981;**199**:865-870

[49] Gianelli G, Manzella A, Puxeddu M. Crustal models of southern Tuscany (Italy). Tectonophysics. 1997;**281**: 221-239

[50] Carmignani L, Decandia FA, Fantozzi PL, Lazzarotto A, Liotta D, Meccheri M. Tertiary extensional tectonics in Tuscany (northern Apennines, Italy). Tectonophysics. 1994; **238**:295-315

[51] Brunet C, Monié P, Jolivet L, Cadet JP. Migration of compression and extension in the Tyrrhenian Sea, insights from 40Ar/39Ar ages on micas along a transect from Corsica to Tuscany. Tectonophysics. 2000;**321**:127-155

[52] Pandeli E, Bertini G, Castellucci P, Morelli M, Monechi S. The sub-Ligurian and Ligurian units of the Monte Amiata geothermal region (South-Eastern Tuscany): New stratigraphic and tectonic data and insight into their relationships with the Tuscan nappe. Bollettino della Società Geologica Italiana Special Volume. 2005;**2005**(3):55-71

[53] Laurenzi MA, Braschi E, Casalini M, Conticelli S. New 40Ar-39Ar dating and revision of the geochronology of the Monte Amiata Volcano, Central Italy. Italian Journal of Geosciences. 2015;**134**: 255-265

[54] Laurenzi MA, La Felice S. New geochronological data on a core sample from David Lazzaretti well. In: Principe C, Lavorini G, Vezzoli L, editors. Il vulcano di Monte Amiata. Nola: Edizioni Scientifiche e Artistiche; 2017. pp. 233-241. ISBN: 978-88-99742-32-4

[55] Brogi A, Liotta D, Meccheri M, Fabbrini L. Transtensional shear zones controlling volcanic eruptions: The middle Pleistocene Monte Amiata volcano (inner northern Apennines, Italy). Terra Nova. 2010;**22**:137-146

[56] Landi P, La Felice S, Petrelli M, Vezzoli L, Principe C. Deciphering textural and chemical zoning of K-feldspar megacrysts from Mt. Amiata volcano (southern Tuscany, Italy): Insights into the petrogenesis and abnormal crystal growth. Lithos. 2019; **324–325**:569-583

[57] La Felice S, Abebe AT, Principe C, Vezzoli L. Petrochemical characters of Monte Amiata volcanics vs stratigraphy. In: Principe C, Lavorini G, Vezzoli L, editors. Il vulcano di Monte Amiata. Nola: Edizioni Scientifiche e Artistiche; 2017. pp. 145-170. ISBN: 978-88-99742-32-4

[58] Rombai C, Trua T, Matteini M. Metamorphic xenoliths and magmatic inclusions in the quaternary lavas of Mt. Amiata (Tuscany, Central Italy):

Inferences for P-T conditions of magma chamber. Atti Società Toscana di Scienze Naturali in Pisa Memorie Serie A. 1995; **102**:21-38

[59] Principe C, Vezzoli L, La Felice S. Stratigraphy and geological evolution of the Monte Amiata volcano. In: Principe C, Lavorini G, Vezzoli L, editors. Il vulcano di Monte Amiata. Nola: Edizioni Scientifiche e Artistiche; 2017. pp. 85-101. ISBN: 978-88-99742-32-4

[60] Principe C, Vezzoli L, La Felice S. Geology of Monte Amiata volcano (Southern Tuscany). Alpine and Mediterranean Quaternary, Special Issue: Quaternary: Past, Present, Future —AIQUA Conference 2018. 2018;**31**: 235-238. ISSN: 2279-7335

[61] Vezzoli L, Principe C. Volcanic facies and emplacement mechanism at Monte Amiata Volcano. In: Principe C, Lavorini G, Vezzoli L, editors. Il vulcano di Monte Amiata. Nola: Edizioni Scientifiche e Artistiche; 2017. pp. 195-213. ISBN: 978-88-99742-32-4)

[62] Principe C, Vezzoli L. Characteristics and significance of intravolcanic saprolite paleoweathering and associate paleosurface in a silicic effusive volcano: The case study of Monte Amiata (middle Pleistocene, Tuscany, Italy). Geomorphology. 2021;**392**:107922. DOI: 10.1016/j.geomorph.2021.107922

[63] Salvador A, editor. International Stratigraphic Guide: A Guide to Stratigraphic Classification, Terminology, and Procedure. 2nd ed. Boulder: Geological Society of America; 1994. p. 214

[64] Cas RAF, Wright JV. Volcanic Successions, Modern and Ancient: A Geological Approach to Processes, Products, and Successions. London: Allen & Unwin; 1987. p. 528

[65] McPhie J, Doyle M, Allen R. Volcanic Textures. Centre for Ore Deposit and Exploration Studies: University of Tasmania; 1993. p. 197

[66] Walker GPL. Lengths of lava flows. Philosophical Transactions of the Royal Society of London A. 1973;**274**: 107-118

[67] La Felice S, Montanari D, Battaglia S, Bertini G, Gianelli G. Fracture permeability and water-rock interaction in a volcanic groundwater reservoir and the concern of its interaction with the geothermal reservoir of Mt. Amiata, Italy. Journal of Volcanology and Geothermal Research. 2014;**284**:95-105

[68] La Felice S, Bertini G, Principe C. Stratigraphy and characterization of the volcanics inside David Lazzaretti well. In: Principe C, Lavorini G, Vezzoli L, editors. Il vulcano di Monte Amiata. Nola: Edizioni Scientifiche e Artistiche; 2017. pp. 213-220. ISBN: 978-88-99742-32-4

[69] Montanari D, La Felice S, Bertini G. Fractures characterisation within recent exploratory wells at Monte Amiata. In: Principe C, Lavorini G, Vezzoli L, editors. Il vulcano di Monte Amiata. Nola: Edizioni Scientifiche e Artistiche; 2017. pp. 221-231. ISBN: 978-88-99742-32-4

[70] Giordano D, Nichols ARL, Dingwell DB. Glass transition temperatures of natural hydrous melts: A relationship with shear viscosity and implications for the welding process. Journal of Volcanology and Geothermal Research. 2005;**142**:105-118

[71] Sparks RSJ, Stasiuk MV, Gardeweg M, Swanson DA. Welded breccias in andesite lavas. Journal of the Geological Society. 1993;**150**:897-902

[72] Rust AC, Manga M, Cashman KV. Determining flow type, shear rate and shear stress in magmas from bubble shapes and orientations. Journal of Volcanology and Geothermal Research. 2003;**122**:111-132

[73] Walker GPL. Pipe vesicles in Hawaiian basaltic lavas: Their origin and potential as paleoslope indicator. Geology. 1987;**15**:84-87

[74] Manga M. Deformation of flow bands by bubbles and crystals. Geological Society of America Special Papers. 2005;**396**:47-54

[75] Morrow N, McPhie J. Mingled silicic lavas in the Mesoproterozoic Gawler Range Volcanics. South Australia: Journal of Volcanology and Geothermal Research. 2000;**96**:1-13

[76] Seaman SJ. Multi-stage magma mixing and mingling and the origin of flow banding in the Aliso Lava Dome, Tumacacori Mountains, southern Arizona. Journal of Geophysical Researches. 1995;**100**:8381-8398

[77] Perugini D, Ventura G, Petrelli M, Poli G. Kinematic significance of morphological structures generated by mixing of magmas: A case study from Salina Island (southern Italy). Earth Planetary Scences Letters. 2004;**222**(3–4):1051-1066

[78] Stevenson RJ, Briggs RM, Hodder APW. Emplacement history of a low-viscosity, fountain-fed pantelleritic lava flow. Journal of Volcanology and Geothermal Research. 1993;**57**:39-56

[79] Gonnermann HM, Manga M. Flow banding in obsidian: A record of evolving textural heterogeneity during magma deformation. Earth Planetary Science Letters. 2005;**236**:135-147

[80] Tuffen H, Dingwell DB, Pinkerton H. Repeated fracture and healing of silicic magma generate flow banding and earthquakes? Geology. 2003;**31**:1089-1092

[81] Anderson SW, Fink JH. Crease structures: Indicators of emplacement rates and surface stress regimes of lava flows. Geological Society of America Bulletin. 1992;**104**:615-625

[82] Lescinsky DT, Merle O. Extensional and compressional strain in lava flows and the formation of fractures in surface crust. In: Manga M, Ventura G, editors. Kinematics and Dynamics of Lava Flows, Geological Society of America Special Paper. Vol. 396. Boulder: Geological Society of America; 2005. pp. 163-179

[83] Farrell J, Karson J, Soldati A, Wysocki R. Multiple-generation folding and non-coaxial strain of lava crusts. Bulletin of Volcanology. 2018;**80**:84. DOI: 10.1007/s00445-018-1258-5

[84] Macdonald GA. Volcanoes. Englewood Cliffs: Prentice Hall Inc.; 1972. p. 501

[85] Bullock LA, Gertisser R, O'Driscoll B. Emplacement of the Rocche Rosse rhyolite lava flow (Lipari, Aeolian Islands). Bulletin of Volcanology. 2018; **80**:48. DOI: 10.1007/s00445-018-1222-4

[86] Fink JH. Gravity instability in the Holocene big and little Glass Mountain rhyolitic obsidian flows, northern California. Tectonophysics. 1980;**66**: 147-166

[87] Baum BA, Krantz WB, Fink JH, Dickinson RE. Taylor instability in rhyolite lava flows. Journal of Geophysical Research. 1989;**94**:5815-5828

[88] Andrews GDM, Kenderes SM, Whittington AG, Isom SL, Brown SR,

Pettus HD, et al. The fold illusion: The origins and implications of ogives on silicic lavas. Earth and Planetary Science Letters. 2021;**553**:116643

[89] Fink JH. Surface folding and viscosity of rhyolite flows. Geology. 1980;**8**:250-254

[90] Finch RH. Block lava. Journal of Geology. 1933;**41**:769-770

[91] Harris AJL, Rowland SK, Villeneuve N, Thordarson T. Pāhoehoe, ʻaʻā, and block lava: An illustrated history of the nomenclature. Bullettin of Volcanology. 2017;**79**:7

[92] Christiansen RL, Lipman PW. Emplacement and thermal history of a rhyolite lava flow near Fortymile canyon, South Nevada. Geological Society of America Bullettin. 1966;**77**:671-684

[93] Schneider JL, Fisher RV. Transport and emplacement mechanisms of large volcanic debris avalanches: Evidence from the northwest sector of cantal volcano (France). Journal of Volcanology and Geothermal Research. 1998;**83**:141-165

[94] Bowman ET, Take WA, Rait KL, Hann C. Physical models of rock avalanche spreading behaviour with dynamic fragmentation. Canadian Geotechnical Journal. 2012;**49**:460-476

[95] Gottsmann J, Dingwell DB. The cooling of frontal flow ramps: A calorimetric study on the Rocche Rosse rhyolite flow, Lipari, Aeolian Islands, Italy. Terra Nova. 2001;**13**:157-164

[96] Latutrie B, Harris A, Médard E, Gurioli L. Eruption and emplacement dynamics of a thick trachytic lava flow of the Sancy volcano (France). Bulletin of Volcanology. 2017;**79**:4. DOI: 10.1007/s00445-016-1084-6

[97] Manley CR, Fink JH. Internal textures of rhyolite flows as revealed by research drilling. Geology. 1987;**15**:549-552

[98] Merle O. Internal strain within lava flows from analogue modelling. Journal of Volcanology and Geothermal Research. 1998;**81**:189-206

[99] Henry CD, Price GJ, Parker DF, Wolff JA. Mid-tertiary silicic alkalic magmatism of trans-Pecos Texas: Rheomorphic tufts and extensive silicic lavas. In: Chapin CE, Zidek J, editors. Field Excursions to Volcanic Terranes in the Western United States, Volume 1: Southern Rocky Mountain Region, New Mexico Bureau of Mines and Mineral Resources Memoir. Vol. 46. Socorro (NM): New Mexico Bureau of Mines and Mineral Resources; 1989. pp. 231-272

[100] Poli G, Frederick A, Ferrara G. Geochemical characteristics of the South Tuscany (Italy) volcanic province. Constraints on lava petrogenesis. Chemical Geology. 1984;**43**:203-221

[101] Le Maitre RW, editor. Igneous rocks. A classification and glossary of terms. Recommendations of the International Union of Geological Sciences Subcommission on the Systematics of Igneous Rocks. 2nd ed. Cambridge: Cambridge University Press; 2002. p. 236

[102] Giordano D, La Felice S, Arzilli F, De Cristofaro SP, Masotta M, Polo L. Effusive acidic volcanism of Monte Amiata: Estimates of pre- and syn-eruptive conditions and volcanological implications. In: Principe C, Lavorini G, Vezzoli L, editors. Il vulcano di Monte Amiata. Nola: Edizioni Scientifiche e Artistiche; 2017. pp. 171-193

[103] Putirka KD. Igneous thermometers and barometers based on plagioclase +

liquid equilibria: Tests of some existing models and new calibrations. American Mineralogist. 2005;**90**:336-346

[104] Putirka KD. Thermometers and barometers for volcanic systems. Review Mineralogy and Geochemistry. 2008;**69**: 61-120

[105] Putirka K, Johnson M, Kinzler R, Walker D. Thermobarometry of mafic igneous rocks based on clinopyroxene-liquid equilibria, 0–30 kbar. Contributions to Mineralogy and Petrology. 1996;**123**:92-108

[106] Masotta M, Mollo M, Freda C, Gaeta M, Moore G. Clinopyroxene–liquid thermometers and barometers specific to alkaline differentiated magmas. Contributions to Mineralogy and Petrology. 2013;**166**:1545-1561

[107] Harrison TM, Watson EB. The behavior of apatite during crustal anatexis: Equilibrium and kinetic considerations. Geochimica et Cosmochimica Acta. 1984;**48**:1467-1477

[108] Ghiorso MS, Gualda GAR. An H_2O - CO_2 mixed fluid saturation model compatible with rhyolite-MELTS. Contributions to Mineralogy and Petrology. 2015;**169**:53. DOI: 10.1007/s00410-015-1141-8

[109] Batini F, Brogi A, Lazzarotto A, Liotta D, Pandeli E. Geological features of the Larderello–Travale and Monte Amiata geothermal areas (southern Tuscany, Italy). Episodes 2003;**26**: 239-244

[110] Marini L, Manzella A. Possible seismic signature of the quartz transition in the lithosphere of Southern Tuscany (Italy). Journal of Volcanology and Geothermal Research. 2005;**148**:81-97

[111] Frondini F, Caliro S, Cardellini C, Chiodini G, Morgantini N. Carbon dioxide degassing and thermal energy release in the Monte Amiata volcanic-geothermal area (Italy). Applied Geochemistry. 2009;**24**:860-875

[112] Sbrana A, Marianelli P, Belgiorno M, Sbrana M, Ciani V. Natural CO_2 degassing in the mount Amiata volcanic–geothermal area. Journal of Volcanology and Geothermal Research. 2020;**397**:106852. DOI: 10.1016/j.jvolgeores.2020.106852

[113] Irsara A, Frezzotti ML, Ghezzo C. Melt and fluid inclusion study in orthopyroxene and plagioclase phenocrysts from M. Amiata Quaternary volcanic complex. Plinius. 1993;**10**: 168-169

[114] Cioni R, Marini L. A Thermodynamic Approach to Water Geothermometry. Heidelberg: Springer; 2020. pp. 415

[115] Giordano D, Russell JK, Dingwell DB. Viscosity of magmatic liquids: A model. Earth Planetary Science Letters. 2008;**271**:123-134

[116] Costa A, Caricchi L, Bagdassarov N. A model for the rheology of particle-bearing suspensions and partially molten rocks. Geochemistry Geophysics Geosystems. 2009;**10**:Q03010. DOI: 10.1029/2008GC002138

[117] Ryan AG, Russell JK, Nichols ARL, Hess KU, Porritt LA. Experiments and models on H2O retrograde solubility in volcanic systems. American Mineralogist. 2015;**100**:774-786. DOI: 10.2138/am-2015-5030

[118] Martin RC. Some field and petrographic features of American and New Zealand ignimbrites. New Zealand

Journal of Geology and Geophysics. 1959;**2**:394-411

[119] Smith RL. Zones and zonal variations in welded ash-flows. In: Shorter Contributions to General Geology 1959, U.S. Geological Survey Professional Paper. Vol. 354-F. Denver (CO): U.S. Geological Survey; 1960. pp. 149-159

[120] Lipman PW, Christiansen RL. Zonal features of an ash-flow sheet in the Piapi canyon formation, southern Nevada. U.S. Geological Survey Professional Paper. Denver (CO): U.S. Geological Survey; 1964;**501-B**:74-78

[121] Allen SR, McPhie J. Phenocryst fragments in rhyolitic lavas and lava domes. Journal of Volcanology and Geothermal Research. 2003;**126**: 263-283

[122] Bertini G, Cappetti G, Dini I, Lovari F. Deep drilling results and updating of geothermal knowledge on the Monte Amiata area. In: Proceedings of the World Geothermal Congress; Florence, Italy. Vol. 2. Den Haag (NL): International Geothermal Association; 1995. pp. 1283-1286

[123] Cashman K. Volatile controls on magma ascent and eruption. In: Sparks RSJ, Hawkesworth CJ, editors. The State of the Planet: Frontiers and Challenges in Geophysics. Washington: American Geophysical Union; 2004. pp. 109-124. DOI: 10.1029/150GM10

[124] Heiken G, Wohletz K. Tephra deposits associated with silicic domes and lava flows. Geological Society of America, Special Paper. 1987;**212**:55-76

[125] Zellmer GF. Some first-order observations on magma transfer from mantle wedge to upper crust at volcanic arcs. The Geological Society of London Special Publication. 2008;**304**:15-31

[126] Castro JM, Dingwell DB, Nichols ARL, Gardner JE. New insights on the origin of flow bands in obsidian. Geological Society of America Special Paper. 2005;**396**:55-66. DOI: 10.1130/0-8137-2396-5.55

[127] Sparks RSJ, Tait SR, Yanev Y. Dense welding caused by volatile resorption. Journal of the Geological Society. 1999; **156**:217-225